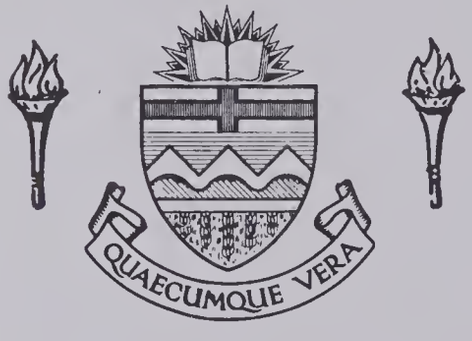

T H E U N I V E R S I T Y O F A L B E R T A

RELEASE FORM

NAME OF AUTHOR Shahul Hameed Meeran Nilar

TITLE OF THESIS A Theoretical Simulation of Interactions in Transmembrane Ionic Channels

DEGREE FOR WHICH THESIS WAS PRESENTED M.Sc.

YEAR THIS DEGREE GRANTED 1983

THE UNIVERSITY OF ALBERTA

A THEORETICAL SIMULATION OF INTERACTIONS IN TRANSMEMBRANE IONIC CHANNELS

by

SHAHUL HAMEED MEERAN NILAR

A THESIS

SUBMITTED TO THE FACULTY OF GRADUATE STUDIES AND RESEARCH

IN PARTIAL FULFILMENT OF THE REQUIREMENTS FOR THE DEGREE

OF MASTER OF SCIENCE

DEPARTMENT OF CHEMISTRY

EDMONTON, ALBERTA

FALL, 1983

THE UNIVERSITY OF ALBERTA

FACULTY OF GRADUATE STUDIES AND RESEARCH

The undersigned certify that they have read, and recommend to the Faculty of Graduate Studies and Research, for acceptance, a thesis entitled A THEORETICAL SIMULATION OF INTERACTIONS IN TRANSMEMBRANE IONIC CHANNELS submitted by SHAHUL HAMEED MEERAN NILAR in partial fulfilment of the requirements for the degree of Master of Science.

To my revered guru

DR. R. A. THURAISINGHAM

Department of Chemistry

University of Colombo

Sri Lanka

ABSTRACT

Reversible interference with the conductance properties of the Sodium channel by anesthetic molecules and preferred interaction with neurotransmitters in the synaptic cleft are two postulated mechanisms of general anesthesia.

In this thesis, both mechanisms have been studied and interaction energies used as the criterion to decide on the preferential binding of the model for the Sodium channel with ions and anesthetic molecules. The interaction energies were evaluated using a 1/R expansion parameterised to reproduce ab-initio energies.

Gramicidin-A dimer was chosen as a model for the Sodium channel and its structure generated by a theoretical conformation analysis. This model was refined in stages by simulating the lipid environment in the membrane with (i) formic acid molecules (ii) formic acid and octane molecules and (iii) formic acid, octane and a chain of water molecules through the channel.

At each stage of improvement of the model, the energy barriers and permeability ratios for the ions under consideration (Li^+, Na^+, K^+, Ca^{2+}) were evaluated and found to be consistent with the experimentally observed two-site binding theory.

The interaction of diethyl ether with the mouth of the channel was found to be preferred over that of a water molecule at the same position. Furthermore, the value of the energy of interaction is in the thermal range and the position of the ether is such as to block the mouth of the channel, thus interfering with the movement of the ions responsible for the depolarisation of the membrane. This hypothesis was tested on the guanidinium ion and the neurotoxins, tetrodotoxin and saxitoxin. Their toxicity is attributed to the large energy of interaction and complete blocking of the channel.

Interactions of diethyl ether with extracellular sodium ions, water and acetylcholine show a definite tendency for the favoured interaction of the ether with the neurotransmitter.

TABLE OF CONTENTS

ABSTRACT.....v

LIST OF TABLES.....ix

LIST OF FIGURES.....x

CHAPTER 1 - INTRODUCTION.....1

1.1 INHIBITORY EFFECTS ON NERVOUS TRANSMISSION.....5

1.2 AIM OF THIS RESEARCH.....7

CHAPTER 2 - THEORETICAL FORMULATION.....12

2.1 INTRODUCTION 12

2.2 DERIVATION OF THE POTENTIAL ENERGY FUNCTION.....14

2.2.1 ELECTROSTATIC CONTRIBUTIONS.....14

2.2.2 INDUCTION ENERGY.....16

2.2.3 DISPERSION ENERGY.....18

2.2.3.1 DERIVATION OF THE DIPOLE-DIPOLE INTERACTION OPERATOR.....19

2.2.3.2 PERTURBATION FORMULATION OF THE DISPERSION ENERGY.....21

2.2.4 SHORT RANGE CONTRIBUTIONS.....23

PAGE

2.2.5 SUMMARY OF THE ANALYTICAL FORMULATION FOR THE INTERSYSTEM POTENTIAL ENERGY.....24

2.2.6 A SEMIEMPIRICAL APPROACH TO THE R^6 COEFFICIENT OF THE DISPERSION CONTRIBUTION - THE SLATER-KIRKWOOD FORMULA.....24

2.3 APPLICATION OF THE 1/R EXPANSION.....28

2.3.1 INTRAMOLECULAR INTERACTIONS.....28

2.3.2 INTERMOLECULAR INTERACTIONS.....31

2.4 METHOD OF CALCULATION.....33

2.5 PROGRAMMING DETAILS.....42

CHAPTER 3 - RESULTS OF THE CALCULATIONS.....44

3.1 GENERATION OF A STRUCTURE FOR THE GRAMICIDIN-A DIMER.46

3.2 IONIC MOVEMENT THROUGH THE PORE OF THE TRANSMEMBRANE CHANNEL.....51

3.3 INTERACTION OF THE CHANNEL WITH MOLECULES.....74

3.3.1 TOXICITY OF TETRODOTOXIN AND SAXITOXIN.....75

3.3.2 INTERACTIONS OF ANESTHETIC MOLECULES.....84

CHAPTER 4 - CONCLUSIONS.....90

REFERENCES 94

LIST OF TABLES

TABLE		PAGE
1	ASSIGNMENT OF ADDITIONAL CLASSES TO ATOMS	36
2	PARAMETERS FOR THE NEW CLASSES OF ATOMS	37
3	BASIS SET FOR Ca^{2+}	39
4	BASIS SETS AND THEIR ENERGIES	40
5	f AND g FACTORS FOR THE IONS	41
6	CHOICE OF HELIX FOR THE BACKBONE OF GRAMICIDIN-A AND THE CORRESPONDING ENERGY	48
7	IONIC RADII	55
8	E_c AND d FOR TRANSPORT THROUGH THE GRAMICIDIN-A DIMER	56
9	E_c AND d FOR TRANSPORT THROUGH THE REFINED MODEL	67
10	E_c AND d FOR TRANSPORT THROUGH THE SOLVATED PORE	73
11	ENERGIES FOR CERTAIN BONDS	84
12	INTERACTION ENERGIES (kJ/MOLE) OF Na^+, ACETYLCHLOLINE, AND WATER WITH DIETHYL ETHER	89

LIST OF FIGURES

FIGURE		PAGE
1	SIDE VIEW OF THE GRAMICIDIN-A MOLECULE	49
2	FRONT VIEW OF THE GRAMICIDIN-A MOLECULE	50
3	LATERAL VIEW OF THE GRAMICIDIN-A DIMER	52
4	FRONT VIEW OF THE GRAMICIDIN-A DIMER	53
5	FRONT AND LATERAL VIEW OF PATH TAKEN BY Li^+	58
6	FRONT AND LATERAL VIEW OF PATH TAKEN BY Na^+	58
7	FRONT AND LATERAL VIEW OF PATH TAKEN BY K^+	59
8	FRONT AND LATERAL VIEW OF PATH TAKEN BY Ca^{2+}	59
9	FRONT VIEW OF GRAMICIDIN-A WITH FORMIC ACID MOLECULES	60
10	CLUSTER OF FORMIC ACID MOLECULES AROUND THE PORE	61
11	LATERAL VIEW OF THE GRAMICIDIN-A DIMER WITH THE SURROUNDING MOLECULES OF FORMIC ACID	63
12	FRONT VIEW OF THE GRAMICIDIN-A DIMER WITH THE SURROUNDING MOLECULES OF FORMIC ACID	64
13	SIDE VIEW OF THE REFINED MODEL OF A GRAMICIDIN-A MONOMER	65
14	THE PORE OF THE REFINED MODEL FOR GRAMICIDIN-A	66
15	SIDE VIEW OF THE REFINED CHANNEL	68
16	FRONT VIEW OF THE REFINED CHANNEL	69

FIGURE PAGE

17 FRONT AND LATERAL VIEW OF THE PATH OF Li^+ THROUGH THE PORE OF THE REFINED MODEL.....71

18 FRONT AND LATERAL VIEW OF THE PATH OF Na^+ THROUGH THE PORE OF THE REFINED MODEL.....71

19 FRONT AND LATERAL VIEW OF THE PATH OF K^+ THROUGH THE PORE OF THE REFINED MODEL.....72

20 STRUCTURES OF TETRODOTOXIN AND SAXITOXIN.....76

21 POSITION OF THE GUANIDINIUM ION AT THE MOUTH OF THE CHANNEL.....78

22 CHANNEL BLOCKING CHARACTERISTIC OF THE GUANIDINIUM ION.....79

23 LATERAL VIEW OF THE INTERACTION OF TETRODOTOXIN WITH THE CHANNEL.....80

24 FRONT VIEW OF THE INTERACTION OF TETRODOTOXIN WITH THE CHANNEL.....81

25 SIDE VIEW OF THE INTERACTION OF SAXITOXIN WITH THE CHANNEL.....82

26 FRONT VIEW OF THE INTERACTION OF SAXITOXIN WITH THE CHANNEL.....83

27 INTERACTION OF DIETHYL ETHER WITH THE CHANNEL PORE.....86

28 PARTIAL BLOCKING OF THE PORE BY THE ETHER.....87

CHAPTER 1 - INTRODUCTION

Nervous transmission is the process by which cells in an organism communicate with each other and the basic cellular units responsible for the transfer of information are called neurons.

A neuron consists of a cell body which contains the cell nucleus. From the cell body, protrusions known as dendrites branch into the extracellular medium. In addition to the dendrites there is a long smooth extension of the cell body known as the axon at the end of which there are little fibres called terminal fibres. Insulation between the axons of two neurons is provided by another type of cell known as the Schwann cell. These cells are wrapped around the axon and the intercellular spaces along the length of the axon are called the nodes of Ranvier. Any branches from the axon occur at such nodal points.

Incoming information from another neuron, known as a signal, is received by the dendrites and conducted along the axon to other parts of the central nervous system (CNS). Communication between neurons is achieved by transmitting these signals across the gaps which separate the neurons. Such gaps are called synapses and, in the majority of the cases, a synapse separates the axon of one neuron from the

dendrite of another. The end of the axon enlarges at the synapse to form a terminal button which is associated with the transmittance of the signal across the synapse.

It has been observed experimentally (1-7) that in the resting state, the outside of an axon is more positive with respect to its interior and the associated potential difference is about -70 mV. A stimulus is required to change this state of the axon and when supplied in the form of an electric pulse causes a depolarisation, in the vicinity of the point of application, across the axonal membrane. This depolarisation, if in excess of a threshold value, has been found to overshoot with the consequent reversal of the polarity across the membrane. This impulse is called the action potential.

The resting state of the neuron is restored after a few milliseconds and the impulse travels along the axon due to the sequential depolarisation of its membrane. At the terminal button of the axon, the impulse is transmitted across the synapse resulting in the depolarisation of the membrane of a second neuron. In this manner, neurons transfer information to various parts of the CNS.

Communication across synapses could be in either of two forms:

(i) chemical transmission

(ii) electrical transmission

As little is known of electrical transmission, the emphasis

has been on chemical transmission which is described below. In this mode of communication, certain types of molecules are associated with the conduction of the signal across the synapse. The terminal button of an axon has spherical structures, known as synaptic vesicles, which contain these transmitter molecules. When an action potential arrives at the axonal terminal, some of the synaptic vesicles release the transmitters into the synaptic cleft. These molecules then diffuse across the synapse and interact with the dendrite membrane of a second neuron. Such interactions with the post-synaptic membrane causes a depolarisation on the second neuron and, therefore, the transmission of the impulse across the synapse.

In a neuron, the concentration of Na^+ in the external medium has been found to be about ten times greater than in the axoplasm, while the reverse holds true for K^+. Hodgkin et al (4-7) observed that the propagation of the nerve impulse corresponded to the change in the permeability of the axonal membrane to Na^+ and K^+.

The arrival of an impulse at a neuron allows the flow of Na^+ into the axoplasm with a simultaneous outflow of K^+. It is this transfer of ions which causes the depolarisation across the membrane. An immediate repolarisation process follows with the Na^+ being driven out of the axoplasm. This restores the neuron to its previous resting state. The restorative mechanism is called the

"Sodium pump" and the energy required to expel the Na^+ is supplied by the hydrolysis of Adenosine triphosphate (ATP). Thus the basic mechanism which causes an impulse and its propagation along the axon is directly associated with the permeability of the axonal membrane to ions.

The passage of an ion, unaided, through a lipid bilayer may not be energetically favourable due to the latter's hydrophobicity and a polar medium spanning the bilayer could help the ion migrate across the membrane. The polypeptide nature of integral membrane proteins satisfy these requirements and they behave as transmembrane channels that facilitate ionic migration. Such channels are selective towards certain ions and the Sodium channel, which allows the transport of Na^+ during nerve impulse, is a very relevant example.

Although the molecular weight of the Sodium channel has been found to be 270 kilo-daltons, its structure is still to be characterised. The average diameter of the channel pore is about 5 Å and conformational changes in the amino acid residues can vary this value according to the size of the ion being transported.

After initiating the pulse on the post-synaptic membrane, the transmitter molecules have no futher use and are destroyed by a related enzyme. After the molecules of the transmitter have been removed, a second impulse can be transmitted through the same intracellular gap.

The release of the neurotransmitter molecules into the synaptic cleft appears to be in small quantized amounts and their diffusion from the pre-synaptic to the post-synaptic membrane determines the direction of the action potential.

1.1 INHIBITORY EFFECTS ON NERVOUS TRANSMISSION

Interference with the initiation or propagation of a nerve impulse will result in the suppression of inter-neuronal communication. Such inhibitory effects could be permanent or temporary depending on the extent of the interference. Usually, molecules which interact with strategic biochemical components necessary for nervous transmission are associated with such effects, examples being neurotoxins and anesthetics.

The interference caused by anesthetics can be regarded as temporary and therefore reversible. That is, after a certain period of time, the inhibitory effect of the anesthetic is diminished and nervous transmission restored to normal levels. Hence the use of anesthetics in surgical applications. Neurotoxins on the other hand, have a more permanent inhibitory influence and in most cases the results are fatal (8).

Many mechanisms have been proposed (9) to explain the inhibitory effects on nervous transmission. Of these, the three that are currently emphasised are:

(i) interference with the initiation of the impulse

(ii) interactions which hinder the diffusion of the transmitter molecules in the synaptic cleft

and

(iii) changes in the structure of the transmitter receptor.

As the initiation of an impulse is directly linked with ionic transport through the Sodium channel, inhibition of nervous transmission may be due to the blocking of the channel by given molecules, thus hindering ionic migration. A logical point of hindrance is the pore of the channel and the interaction of the inhibitor molecules with the mouth of the pore could be one of the factors responsible for this interference.

Another possibility is the complexing of the inhibitor molecules with chemical transmitters like acetylcholine. The second hypothesis implies that such interactions should be more favourable than the corresponding interactions with other molecular and ionic species in the synaptic cleft. Further, the diffusion of a complexed transmitter towards the receptor on the post-synaptic membrane is hindered and thus, the probability of depolarising the second neuron significantly reduced.

Each neurotransmitter has its associated receptor on the post-synaptic membrane and interactions between the two which are responsible for the transmission of the impulse,

take place at strategic points on the receptor. The blocking of such points by anesthetics or toxins diminishes the transmitter-receptor interactions responsible for nervous transmission. For example, the toxicity of curare is believed to be due to the blocking of the active sites of the receptor on the post-synaptic membrane.

The brief outlines of each of the three mechanisms presented above give an indication of some of the possible interactions responsible for the anesthetic or toxic properties of some molecules. The reduction of inter-neuronal communication may be due to any one or more of the processes described by the postulated mechanisms. From a chemical point of view, the third mechanism is more difficult to investigate, as very little is known about the receptor sites on the post-synaptic membrane. In the case of the first two mechanisms the structural details of the systems involved are better understood and can be investigated by suitable simulations of the molecular species and related environments.

1.2 AIM OF THIS RESEARCH

In this thesis an attempt has been made to understand some of the possible molecular interactions which are responsible for the inhibition of nervous transmission. The first two of the three proposed mechanisms were studied

using theoretical simulation techniques. The energy of interaction between two systems under investigation was used as the criterion to decide on their preferential binding. The mode of evaluation of this energy is described briefly in the next subsection.

As the Sodium channel is not structurally fully characterised, a suitable model based on available experimental information was used instead. The energy gradients for the passage of some alkali and alkali earth ions through the model channel were determined and found to be in good agreement with experiment. The toxicity of the neurotoxins, tetrodotoxin and saxitoxin, was studied by determining the nature of their interaction with the pore of the channel. Further, the position of the toxins was found to block the pore of the channel, interfering with the transport of ions. This observation indicates that such toxins hinder the depolarisation of the membrane and hence nervous transmission.

A similar study on the anesthetic nature of diethyl ether indicated that the energy of interaction of the ether with the mouth of the pore was in the thermal range. Such interactions are relatively weak and can be overcome by molecular collisions and conformational changes in the systems concerned - a prerequisite for the temporary inhibition of nervous transmission as observed in anesthesia.

The second postulated mechanism was studied next. Extracellular Na^+, acetylcholine and water were chosen as some of the species in the synaptic cleft. Molecules of diethyl ether were clustered around each of the species mentioned above. The interaction energy of each ether molecule with the second entity was evaluated. As postulated, the trend in these energies showed a definite preference for the interaction of the ether with acetylcholine than with Na^+ or water.

1.3 MODE OF EVALUATION OF INTERACTION ENERGIES

A quantum mechanical treatment of a system of interest requires the solution of the Schrodinger equation

$$H\psi = E\psi \qquad 1.2.1$$

where H is the Hamiltonian operator which includes all the interactions in the system, E and ψ being the corresponding eigenvalue and eigenfunction, respectively.

At present, exact solutions to this equation are available for hydrogen-like systems only and approximations are required for the treatment of larger systems. Most molecules involved in biochemical phenomena have many nuclei and electrons and the approximations invoked are, in many cases, drastic. The results obtained from such calculations

are questionable as the approximations and models used may have very little relevance to the process under investigation.

The Born-Oppenheimer approximation (10) which separates the nuclear and electronic parts of the total wave function ψ as

$$\psi = \psi_{electronic} \cdot \psi_{nuclear} \qquad 1.3.2$$

is a basis of most molecular electronic calculations. Keeping the nuclear geometry fixed, the electronic energy of the system and its approximate wave function can be evaluated.

Ab-initio calculation of the electronic energy is usually based on the Hartree-Fock-Roothan (11) self-consistent field technique. The amount of computer time required for such a treatment increases as a function of the number of electrons to the fourth power. This has been the main drawback in the rigorous application of this method to large systems. The cost of such calculations will be phenomenal in a meaningful treatment of biomolecules and to overcome this disadvantage, semiempirical methods have been used with varying degrees of success.

The method of calculation used in this thesis to evaluate the interaction energy between two systems A and B is based on the theory of weak interactions. An assumption

in this theory is that the wave functions of the constituent systems are not altered during interaction and therefore, a multipolar expansion of the potential of interaction is possible. Such a multipolar expansion expresses the interaction between A and B as a function of the reciprocal of the distance separating the various atoms and is referred to as a 1/R expansion.

The semiempirical method used here evaluates the interaction energy from a truncated 1/R expansion parameterised to reproduce ab-initio calculations. The details of the method of calculation are given in Chapter 2.

The reasons behind the choice of certain molecules for the simulation of the biological systems and environments and the results obtained from the application of the semiempirical formulation are presented in Chapter 3. Figures of the interacting systems are given to emphasise certain salient features of the results.

General conclusions on the applicability and improvements to the model are discussed in the final chapter.

CHAPTER 2 - THEORETICAL FORMULATION

2.1 INTRODUCTION

In order to evaluate the interaction energy between two systems A and B, a suitable potential energy function V(r) has to be chosen. This function, which measures the interaction between A and B, will describe the difference in the total energy of the system at a distance r from its value when A and B are infinitely separated. Thus E_{total}, the total energy of the composite system, is given by

$$E_{total} = E_A + E_B + V(r) \qquad 2.1.1$$

where E_X (X = A, B) is the energy of the isolated system X. As the distance separating A and B increases, the influence of each system on the other decreases. Hence the values of V(r) decreases with r and at infinite separation

$$E_{total} = E_A + E_B \qquad 2.1.2$$

V(r) can be regarded as a cumulative effect of attractive and repulsive contributions between the particles constituting the systems. For chemical purposes, the particles are the electrons and protons of the atoms making

up A and B.

For theoretical purposes, the energy of interaction ΔE can be divided into

(i) Long range contributions

(ii) Short range contributions.

At long range, the overlap of the wave functions is assumed to be small and thus the wave function ψ of the composite system can be expressed as a product $\psi_A\psi_B$ of the wave functions of the isolated systems (12-15). However, for interactions at short distances, such an assumption about the wave function of the total system is not valid as the overlap of the electron clouds is significant. In such a case, the total wave function is an antisymmetrised product of all the electrons in the composite system.

The long range contributions to ΔE can be subdivided into an electrostatic component $\Delta E_{electrostatic}$, an induction contribution ΔE_{ind} and a term ΔE_{disp} due to the dispersion energy. The physical meaning of each of these subdivisions is described below.

At a finite distance r separating A and B, the interaction of the charges on one system with that of the other introduces the electrostatic component $\Delta E_{electrostatic}$. The collection of charges on A induces a field on B, and vice-versa. The field induced by one system interacts with the other system and this component of ΔE is termed the induction energy ΔE_{ind}. The electron clouds in a

system are in continuous motion. Even if the interacting systems have no permanent dipole moment, they will possess an instantaneous dipole moment. The interaction between the two instantaneous dipoles produces the dispersion energy component, ΔE_{disp}, of ΔE.

Thus ΔE can be regarded as being composed of the following contributions:

$$\Delta E = \Delta E_{electrostatic} + \Delta E_{ind} + \Delta E_{disp} + \Delta E_{short\text{-}range} \qquad 2.1.3$$

2.2 DERIVATION OF THE POTENTIAL ENERGY FUNCTION

2.2.1 ELECTROSTATIC CONTRIBUTIONS

The potential ϕ_P at a point P due to charges Q_1 and Q_2 arranged about a center of mass O is given by

$$\phi_P = \frac{1}{4\pi\varepsilon_0} \left[\frac{Q_1}{r_1} + \frac{Q_2}{r_2}\right] \qquad 2.2.1.1$$

where ε_0 is the permittivity in free space and r_1, r_2, the distances of P from Q_1 and Q_2, respectively.

If θ is the positive angle $\overline{OP}$ makes with $\overline{Q_1Q_2}$ and z_1, z_2 the distances of Q_1 and Q_2 from O,

$$\phi_P = \frac{1}{4\pi\varepsilon_0}\left[\frac{Q_1}{[r^2+z_1^2+2rz_1\cos\theta]^{1/2}} + \frac{Q_2}{[r^2+z_2^2-2rz_2\cos\theta]^{1/2}}\right] \qquad 2.2.1.2$$

Assuming $r >> z_1$, z_2 and expanding in powers of z_1/r and z_2/r using the binomial expansion,

$$\phi_P = \frac{1}{4\pi\varepsilon_0}\left[\frac{Q_1+Q_2}{r} + \frac{(Q_2z_2-Q_1z_1)\cos\theta}{r^2} + \frac{(Q_1z_1^2+Q_2z_2^2)}{2r^3}(3\cos^2\theta-1) + \ldots\right] \qquad 2.2.1.3$$

Substituting

$$Q = Q_1 + Q_2,$$

$$\mu = Q_2z_2 - Q_1z_1$$

and

$$H = Q_1z_1^2 + Q_2z_2^2$$

one obtains

$$\phi_P = \frac{1}{4\pi\varepsilon_0}\left[\frac{Q}{r} + \frac{\mu\cos\theta}{r^2} + \frac{H}{2r^3}(3\cos^2\theta-1) + \ldots\right] \qquad 2.2.1.4$$

Consider a second charge distribution (Q_1', Q_2') with centre of mass S. The relative orientation of (Q_1', Q_2') with respect to (Q_1, Q_2) is defined as follows:

(i) θ_1 and θ_2 are the angles made by OQ_1' and OQ_2' with OS repectively.

(ii) z_1 and z_2 are distances of Q_1' and Q_2' from S and

(iii) ϕ is the angle, measured in an anti-clockwise sense, made by (Q_1', Q_2') with (Q_1, Q_2) about the line OS.

The electrostatic component, $\Delta E_{electrostatic}$ of ΔE is given by

$$\Delta E_{electrostatic} = Q_1'\phi(r_1') + Q_2'\phi(r_2') \qquad 2.2.1.5$$

Using equation 2.2.1.4 and substituting

$$Q' = Q_1' + Q_2'$$
$$\mu' = Q_2'z_2' - Q_1'z_1'$$
$$H' = Q_2'z_2'^2 + Q_1'z_1'^2,$$

one obtains

$$\Delta E_{electrostatic} = \frac{1}{4\pi\varepsilon_0}\left[\frac{QQ'}{r} + \frac{1}{r^2}(Q'\mu\cos\theta_1 - Q\mu'\cos\theta_2) - \frac{\mu\mu'}{r^3}(2\cos\theta_1\cos\theta_2 - \sin\theta_1\sin\theta_2\cos\phi) + \frac{1}{2r^3}\{Q H'(3\cos^2\theta_2 - 1) + Q' H (3\cos^2\theta_1 - 1)\} + \ldots\right] \qquad 2.2.1.6$$

2.2.2. INDUCTION ENERGY

Suppose E is the static electric field produced by system A and μ_{ind}, the induced dipole moment of system B due to E. Then, by definition,

$$\mu_{ind} = \alpha E \qquad 2.2.2.1$$

and

$$\Delta E_{ind} = -\int_0^E \alpha \varepsilon d\varepsilon = -\tfrac{1}{2}\,\alpha\, E^2 \qquad 2.2.2.2$$

where α is the static polarisability of B.

The magnitude ε of the induced energy at P, at a distance r from O, is given by

$$\varepsilon = \left[\left(\frac{\partial \phi_P}{\partial r}\right)^2 + \frac{1}{r}\left(\frac{\partial \phi_P}{\partial \theta}\right)^2\right]^{1/2} \qquad 2.2.2.3$$

which becomes, taking into account equation 2.2.1.4,

$$\varepsilon = \frac{1}{4\pi\varepsilon_0}\left[\frac{Q^2}{r^4} + 4\mu\,\frac{Q\mathrm{Cos}\theta_1}{r^5} + \frac{\mu^2}{r^6}\,(3\mathrm{Cos}^2\theta_1+1) + \ldots\right]^{1/2} \qquad 2.2.2.4$$

Substituting equation 2.2.2.4 in 2.2.2.2, the induced energy, ΔE_{ind}, of the second system due to the field of the first one is

$$\Delta E_{ind} = -\frac{1}{2}\,\frac{\alpha'}{(4\pi\varepsilon_0)^2}\left\{\frac{Q^2}{r^4} + 4\mu\,\frac{Q\mathrm{Cos}\theta_1}{r^5} + \frac{\mu^2}{r^6}\,(3\mathrm{Cos}^2\theta_1+1) + \ldots\right\} \qquad 2.2.2.5$$

where α' is the polarisability of the second system.

As in the case of electrostatic contributions, the total induced energy E_{ind}, when A and B interact is

$$\Delta E_{ind} = \frac{1}{(4\pi\varepsilon_o)^2}\left[-\tfrac{1}{2}\left(\frac{\alpha' Q^2 + \alpha Q'^2)}{r^4} - 2\left(\frac{\mu Q\alpha' \cos\theta_1 + \mu' Q' \alpha \cos\theta_2)}{r^5}\right.\right.$$
$$\left.\left. - \frac{\{\mu^2\alpha'(3\cos^2\theta_1 + 1) + \mu'\alpha(3\cos^2\theta_2 + 1)\}}{2r^6} - \ldots\right]\right. \qquad 2.2.2.6$$

2.2.3 DISPERSION ENERGY

As stated in section 2.1, the dispersion energy component ΔE_{disp} of ΔE is due to the interaction of the instantaneous dipole moments of A and B. Thus, ΔE_{disp} will be given by

$$\Delta E_{disp} = \langle\psi|W_{dd}|\psi\rangle \qquad 2.2.3.1$$

where ψ is the wave function for the composite system and W_{dd} , the quantum mechanical operator for dipole-dipole interactions.

Expressing ψ as $\psi_A\psi_B$ (section 2.1), at long range separations, one has

$$\Delta E_{disp} = \langle\psi_A\psi_B|W_{dd}|\psi_A\psi_B\rangle \qquad 2.2.3.2$$

2.2.3.1 DERIVATION OF THE DIPOLE-DIPOLE INTERACTION OPERATOR

The potential ϕ_i at a point P_i due to a charge e_i at Q_i is given by

$$\phi_i = \frac{e_i}{R_i} \qquad 2.2.3.1.1$$

where,

$$\begin{aligned} R_i &= |r_i - r_Q| \\ r_i &\equiv OP_i \\ r_Q &\equiv OQ \end{aligned} \qquad 2.2.3.1.2$$

with respect to an origin O. Expansion of ϕ_i using the Taylor-Maclaurin expansion yields

$$\phi_i = \frac{e_i}{r_i} + e_i \sum_j^3 x_{Q,j} \left[\frac{\partial}{\partial x_{Q,j}} \left(\frac{1}{R_i} \right) \right]_{R_i=r_i} + \tfrac{1}{2} q_i \sum_{j,k}^3 x_{Q,j} x_{Q,k} \left[\frac{\partial^2}{\partial x_{Q,k} \partial x_{Q,j}} \left(\frac{1}{R_i} \right) \right]_{R_i=r_i} + \qquad 2.2.3.1.3$$

Differentiating equation 2.2.3.1.2 with respect to the Cartesian components, yields

$$\frac{\partial f(R_i)}{\partial x_{Q,j}} = - \frac{\partial f(R_i)}{\partial x_{P,j}} \qquad 2.2.3.1.4$$

and substituting equation 2.2.3.1.4 in equation 2.2.3.1.3, the dipole potential $\phi^{(2)}$ due to N charged particles becomes

$$\phi^{(2)} = \sum_{i=1}^{N} e_i \sum x_{Q,j} \frac{\partial}{\partial x_{p,j}} \left(\frac{1}{r}\right)$$

$$= - p \cdot \nabla \left(\frac{1}{r}\right) \qquad 2.2.3.1.5$$

$$= \frac{p \cdot r}{r^3}$$

where p is the dipole moment of the system, defined as

$$p = \sum_{i=1}^{N} e_i \sum_{j=1}^{3} x_{Q,j} \qquad 2.2.3.1.6$$

The electric dipole field vector $E^{(2)}$ is given by

$$E^{(2)} = - \nabla \phi^{(2)}$$

$$= -\nabla \frac{(p \cdot r)}{r^3}$$

$$= - \frac{1}{r^3} \nabla(p \cdot r) - (p \cdot r) \nabla\left(\frac{1}{r^3}\right)$$

$$= - \frac{p}{r^3} + (p \cdot r) \frac{3r}{r^5}$$

$$= \frac{1}{r^5} [3(p \cdot r)r - pr^2] \qquad 2.2.3.1.7$$

If the interacting systems A and B, have dipoles p_A and p_B such that

$$p_A = e r_A \qquad 2.2.3.1.8$$

and

$$p_B = er_B \qquad 2.2.3.1.9$$

where r_X (X = A, B) is the distance of the electron cloud from nucleus X, the dipole-dipole interaction energy E_{dd} is then given by

$$E_{dd} = \frac{e^2}{r^3} [r_A \cdot r_B - 3(r_A \cdot n)(r_B \cdot n)] \qquad 2.2.3.1.10$$

where n is the unit vector in the direction $\overline{AB}$.

The dipole-dipole interaction operator W_{dd} is then

$$W_{dd} = \frac{e^2}{r^3} [x_A x_B + y_A y_B - 2z_A z_B] \qquad 2.2.3.1.11$$

2.2.3.2 PERTURBATION FORMULATION OF THE DISPERSION ENERGY.

The first and second order perturbation changes to the energy of the systems A and B, $E_0^{(1)}$ and $E_0^{(2)}$ are given by

$$E_0^{(1)} = \langle \psi_A \psi_B | W_{dd} | \psi_A \psi_B \rangle \qquad 2.2.3.2.1$$

and

$$E_0^{(2)} = -\sum_v \sum_u \frac{|\langle \psi_A \psi_B | W_{dd} | \psi_{A_u} \psi_{B_v} \rangle|^2}{E_{A_u B_v} - E_{AB}} \qquad 2.2.3.2.2$$

where E_{AB} is the total energy of the isolated systems A and B obtained by separate solution of their Schrodinger equations and $E_{A_u B_v}$ is the sum of the energies of A and B in the states u and v.

The dispersion contribution to the energy, correct to second order, is:

$$\Delta E_{disp} = E_0^{(1)} + E_0^{(2)} \qquad 2.2.3.2.3$$

Assuming that ψ is spherically symmetric, $E_0^{(1)} = 0$ from equations 2.2.3.2.1 and 2.2.3.1.11 one obtains

$$\Delta E_{disp} = E_0^{(2)} \qquad 2.2.3.2.4$$

From equations 2.2.3.1.11 and 2.2.3.2.2

$$\begin{aligned} \Delta E_{disp} = -\frac{e^2}{r^6} \sum_u \sum_v \{ & \langle \psi_A | x_A | \psi_{A_u} \rangle \langle \psi_B | x_B | \psi_{B_v} \rangle \\ & + \langle \psi_A | y_A | \psi_{A_u} \rangle \langle \psi_B | y_B | \psi_{B_v} \rangle \\ & -2 \langle \psi_A | z_A | \psi_{A_u} \rangle \langle \psi_B | z_B | \psi_{B_v} \rangle \}^2 / [E_{A_u B_v} - E_{AB}] \end{aligned} \qquad 2.2.3.2.5$$

Inclusion of dipole-quadrupole interactions and quadrupole-quadrupole interactions will include higher order terms in r.

In general, the dispersion energy, ΔE_{disp} can be expressed as

$$E_{disp} = \frac{C_6}{r^6} + \frac{C_8}{r^8} + \frac{C_{10}}{r^{10}} + \ldots \qquad 2.2.3.2.6$$

where, in particular, C_6/r^6 is given by equation 2.2.3.2.5.

2.2.4 SHORT RANGE CONTRIBUTIONS

In the short range region, there is considerable overlap of the wave-functions of the two systems A and B. Hence, the perturbation treatment as presented in 2.2.3 and the multipolar expansions used to derive the long range contributions are not strictly valid.

In order to overcome these difficulties, an empirical potential form is used to represent these short range forces. The functional form used generally is the Lennard-Jones (6-12) (16) given as

$$\Delta E_{short\text{-}range} = \varepsilon \{(\frac{r_n}{r})^{12} - 2(\frac{r_n}{r})^6\} \qquad 2.2.4.1$$

where r_n and ε are the equilibrium distance for the pair-potential interaction and ε, the depth of the potential energy minimum with respect to the energy of the systems at infinite separation.

2.2.5 SUMMARY OF THE ANALYTICAL FORMULATION FOR THE INTERSYSTEM POTENTIAL ENERGY

From subsections 2.2.1 - 2.2.4, the interaction energy ΔE can be expressed as:

$$\Delta E = \frac{A_1}{R} + \frac{A_2}{R^2} + \frac{A_3}{R^3} + \frac{A_4}{R^4} + \frac{A_6}{R^6} + \frac{A_8}{R^8} + \frac{A_{10}}{R^{10}} + \frac{A_{12}}{R^{12}} + \ldots \qquad 2.2.5.1$$

where the A_i's are coefficients associated with the corresponding powers of R.

For practical applications, such an equation is of little use and a semiempirical evaluation of some of the coefficients and suitable truncation of the multipolar expansion is required.

2.2.6 A SEMI-EMPIRICAL APPROACH TO THE R^6 COEFFICIENT OF THE DISPERSION CONTRIBUTION - THE SLATER-KIRKWOOD FORMULA[17]

The dispersion contribution, ΔE_{disp}, to the interaction between spherically symmetric atoms (see equation 2.2.3.2.5) may be written (in atomic units) as

$$\Delta E_{disp} = -\frac{6}{r^6} \sum_u \sum_v \frac{\langle \psi_A | z_A | \psi_{A_u} \rangle^2 \langle \psi_B | z_B | \psi_{B_v} \rangle^2}{(E_{A_u} E_{B_v} - E_{AB})} \qquad 2.2.6.1$$

$$= -\frac{6}{r^6} \sum_u \sum_v \frac{z_{A_u}^2 \, z_{B_v}^2}{(E_A(u,0) + E_B(v,0))} \qquad 2.2.6.2$$

with

$$z_{A_u} = \langle \psi_A | z_A | \psi_{A_u} \rangle$$

$$z_{B_v} = \langle \psi_B | z_B | \psi_{B_v} \rangle$$

$$E_{A_u B_v} - E_{AB} = E_{A_u} + E_{B_v} - E_A - E_B = E_{A(u,0)} + E_B(v,0) \qquad 2.2.6.3$$

where $E_x(m,0)$ represents the energy of atom X in state m referred to the energy of its ground state (X = A, B; m = u,v).

A simplification of this expression may be achieved, as discussed below, through its relationship to the integral

$$I = \int_{-\infty}^{\infty} \frac{E_A(u,0) \, z_{A_u}^2 E_B(v,0) z_{B_v}^2}{(E_A(u,0)^2 + t^2)(E_B(v,0)^2 + t^2)} \, dt \qquad 2.2.6.4$$

The integral I can be expressed as

$$I = \lim_{R \to \infty} \int_{-R}^{R} \frac{E_A(u,0) \, z_{A_u}^2 \, E_B(v,0) \, z_{B_v}^2}{(E_A(u,0)^2 + t^2)(E_B(v,0)^2 + t^2)} \, dt \qquad 2.2.6.5$$

$$+ \int_{\Gamma} \frac{E_A(u,0) \, z_{A_u}^2 \, E_B(v,0) \, z_{B_v}^2}{(E_A(u,0)^2 + t^2)(E_B(v,0)^2 + t^2} \, dt$$

where Γ is a semicircle above the x axis having the line (-R, +R) as diameter. In the limit as $R \to \infty$, the second

term in equation 2.2.6.5 vanishes and, using the theorem of residues, one obtains

$$I = \frac{\pi \, z_{A_u}^{\,2} \, z_{B_v}^{\,2}}{(E_A(u,0) + E_B(v,0))} \qquad 2.2.6.6$$

Comparing equations 2.2.6.4 and 2.2.6.6 with equation 2.2.6.2 one obtains

$$\Delta E_{disp} = \frac{-6}{\pi r^6} \sum_u \sum_v \int_{-\infty}^{\infty} \frac{E_A(u,0)E_B(v,0)z_{A_u}^{\,2}z_{B_v}^{\,2}}{(E_A(u,0)+t^2)(E_B(v,0)+t^2)} \, dt \qquad 2.2.6.7$$

Making use of the formula for the frequency dependent polarisability $P(\nu)$ of an atom (18), namely

$$P(\nu) = 2 \sum_u \frac{E_A(u,0) \, z_{A_u}^{\,2}}{(E_A(u,0)-(h\nu)^2)}$$

and introducing an imaginary frequency $s = ih\nu$, the above equation can be written as

$$P(s) = 2 \sum_u \frac{E_A(u,0) \, z_{A_u}^{\,2}}{(E_A(u,0) + s^2)} \qquad 2.2.6.8$$

Substitution of equation 2.2.6.8 in 2.2.6.7 yields

$$\Delta E_{disp} = \frac{-3}{\pi r^6} \int_0^{\infty} P_A(s) \, P_B(s) \, ds \qquad 2.2.6.9$$

The analytical expression of Mavroyannis et al (19) expresses $P_A(s)$ as

$$P_A(s) = \frac{D^2}{d^2+s^2} \qquad 2.2.6.10$$

The constants D and d are adjusted so as to reproduce the static polarisability α as

$$\frac{D}{d^2} = \alpha \qquad 2.2.6.11$$

and the polarisability at large frequencies as

$$D = \frac{\sum_w f_{0w}}{4\pi^2} \qquad 2.2.6.12$$

where f_{0w} is the oscillator strength for the transition from the state 0 to state w.

Using the Thomas-Reiche-Kuhn rule, which equates the total oscillator strength to the total number of electrons on atom A, and equations 2.2.6.11 and 2.2.6.12, the dispersion energy component of the interaction energy can be written as

$$\Delta E_{disp} = \frac{3}{\pi r^6} \int_0^\infty \frac{D_A D_B}{(d_A^2+s^2)(d_B^2+s^2)}\, ds \qquad 2.2.6.13$$

After evaluating the integral in the above equation, one obtains

$$\Delta E_{disp} = \frac{-3}{2r^6} \frac{\alpha_A \alpha_B}{[(\frac{\alpha_A}{N_A})^{1/2} + (\frac{\alpha_B}{N_B})^{1/2}]} \qquad 2.2.6.14$$

Equation 2.2.6.14 is referred to as the Slater-Kirkwood formula for the dispersion energy contribution.

2.3. APPLICATION OF THE 1/R EXPANSION

The 1/R expansion has been applied in the evaluation of interaction energies for

(i) Intramolecular interactions

and

(ii) Intermolecular interactions

2.3.1 INTRAMOLECULAR INTERACTIONS

In the method of Scheraga et al (20-24), the conformational energy of a polypeptide chain is considered as a function of the various dihedral angles and evaluated as a sum of the leading terms of the coulombic, dispersion and repulsion contributions derived in the foregoing sub-sections. A torsional energy contribution for rotations about dihedral angles and a semiempirically fitted hydrogen-bonding energy term are also included. A result of this formulation was the estimation of parameters to be used in empirical potential energy functions for pair-wise additive interactions.

The coulombic term E^C is given by

$$E^C = \sum_i \sum_j q_i q_j / D r_{ij} \qquad 2.3.1.1$$

where q_k is the electronic charge on atom k calculated by the complete neglect of differential overlap method (25), D is an effective dielectric constant given a value 2 and r_{ij}, the distance between atoms i and j.

The repulsion and dispersion energy terms, together called the non-bonding term, are evaluated using a Lennard-Jones (16) function as

$$E_{\text{Non-bonded}} = \sum_i \sum_j (A_{k\ell}/r_{ij}^{12} - C_{k\ell}/r_{ij}^{6}) \qquad 2.3.1.2$$

where $C_{k\ell}$ is obtained using the Slater-Kirkwood formula (2.2.6.14).

The Lennard-Jones formula for the interaction between two similar atoms k gives A_{kk} as

$$A_{kk} = -\varepsilon^{kk} \langle r_g^{kk} \rangle^{12} \qquad 2.3.1.3$$

with r_g^{kk} and ε defined in section 2.2.4. The brackets enclosing r_g^{kk} denote an average value, i.e.,

$$\langle r_g^{k\ell} \rangle = (\langle r_g^{kk} \rangle + \langle r_g^{\ell\ell} \rangle)/2 \qquad 2.3.1.5$$

with

$$\varepsilon_{k\ell} = -C^{k\ell}/2\langle r_g^{k\ell}\rangle^6 \qquad 2.3.1.6$$

one obtains

$$A^{k\ell} = -\varepsilon^{k\ell} \langle r_g^{k\ell}\rangle^{12} \qquad 2.3.1.7$$

The hydrogen bonding contributions E_{HB} are given (21) by:

$$E_{HB} = \sum_k \sum_\ell (A'_{H\ldots X} / r^{12}_{H\ldots X} - B'_{H\ldots X}/r^{10}_{H\ldots X}) \qquad 2.3.1.8$$

where the summation includes only the hydrogen-bonded pairs. The constants $A'_{H\ldots X}$ and $B'_{H\ldots X}$ are evaluated (21) by fitting the hydrogen bonding contribution of linear bonded dimers evaluated by the complete neglect of differential overlap method to a $(R^{-10} + R^{-12})$ expansion.

For rotations about a peptide bond, the torsional energy term (in kJ/mole) is evaluated using:

$$E_{tor} = \left(\frac{4.828}{2}\right) (1-\mathrm{Cos}2\theta) \qquad 2.3.1.9$$

where θ is the torsional angle, while E_{tor} for rotations of the side chain dihedral angles (x) is given by:

$$E_{tor} = (U_0/2)\ (1 \pm \text{Cos}\ 3x) \qquad 2.3.1.10$$

where

U_0

$\equiv$ 0.6453 kJ/mole for rotations about C-C saturated bonds
$\equiv$ 0.1434 kJ/mole for rotations about C-O hydroxyl bonds
$\equiv$ 0.4302 kJ/mole for rotations about C-N amine bonds

2.3.2 INTERMOLECULAR INTERACTIONS

From section 2.2.5, the energy of interaction ΔE_{AB} between two molecules A and B can be evaluated as a sum of individual interatomic pair potentials according to the equation

$$\Delta E_{AB} = \sum_{a \in A} \sum_{b \in B} \left[\frac{A_{ab}}{R_{ab}} + \frac{B_{ab}}{R_{ab}^2} + \frac{C_{ab}}{R_{ab}^3} + \ldots\right] \qquad 2.3.2.1$$

where A_{ab}, B_{ab}, C_{ab}, can be obtained by comparison with equations 2.2.1.6, 2.2.2.6, 2.2.4.1 and 2.2.6.14. The form of equation 2.2.5.1 makes its practical applicability and usefulness questionable. For computational purposes, the first term in each of the contributions to ΔE_{AB} are used to evaluate the energy of interaction.

A particular example is the potential energy function of Minicozzi and Bradley (26) which approximates ΔE_{AB} as:

$$\Delta E_{AB} = \sum_{a \in A} \sum_{b \in B} \left(\frac{A_{ab}}{R_{ab}} + \frac{B_{ab}}{R_{ab}^{4}} + \frac{C_{ab}}{R_{ab}^{6}} + \frac{D_{ab}}{R_{ab}^{12}} \right) \qquad 2.3.2.2$$

where

$$A_{ab} \equiv Q_a Q_b \qquad 2.3.2.3$$

$$B_{ab} \equiv -\tfrac{1}{2} \left(\alpha_a Q_b^{2} + \alpha_b Q_a^{2} \right) \qquad 2.3.2.4$$

$$C_{ab} \equiv -\, 3/2 \; \alpha_a \alpha_b \left| \left[\left(\frac{\alpha_a}{n_a} \right)^{\frac{1}{2}} + \left(\frac{\alpha_b}{n_b} \right)^{\frac{1}{2}} \right] \right. \qquad 2.3.2.5$$

$$D_{ab} \equiv D_a D_b \; (27)$$

Q_x, α_x, r_x and D_x are, respectively, the electronic charge, static polarisability, effective number of electrons and a semiempirical parameter associated with atom X.

Another example of a 1/R expansion is that reported by Clementi et al (28-30) which expresses the interaction energy ΔE_{AB} as

$$\Delta E_{AB} = \sum_{a \in A} \sum_{b \in B} \left(\frac{A_{ab}}{R_{ab}} + \frac{B_{ab}}{R_{ab}^{6}} + \frac{C_{ab}}{R_{ab}^{12}} \right) \qquad 2.3.2.6$$

The above equation breaks down the interaction energy into pairwise contributions and the constants A_{ab}, B_{ab} and C_{ab} are evaluated by fitting the interaction energy between two systems A and B calculated in the self-consistent field (SCF) approximation to equation 2.3.2.6. A disadvantage in a formulation of this type is that each atom pair a,b has a set of constants (A_{ab}, B_{ab}, C_{ab}) associated with it. Many

such sets have to be evaluated for the interaction of large molecules. This reduces the practical applicability of the scheme.

In order to overcome this drawback, an atom in a molecule is assigned to classes based on its net atomic charge and molecular orbital valence state (MOVS) (31). The MOVS represent the one-center contributions to the SCF energy and reflect the environment of the atoms in a molecule.

In references (28-30), the interaction energy for each of the twenty-six amino acids with water have been calculated. The water molecule was placed at different positions so as to describe the interaction between the two systems as completely as possible.

The atoms in each amino acid are assigned to their classes and the constants (A, B, C) evaluated for the interactions of the atoms in each class with the hydrogen and oxygen of water.

2.4 METHOD OF CALCULATION

In this thesis, the potential energy function of Minicozzi and Bradley (26), modified at the R^4 and R^6 terms was used to evaluate the interaction energy between two systems A and B. The expression used for the calculation of ΔE_{AB} was:

$$\Delta E_{AB} = \sum_{a\epsilon A} \sum_{b\epsilon B} \{\frac{Q_a Q_b}{R_{ab}} - \tfrac{1}{2} (\frac{f_a \alpha_a Q_b^2 + f_b \alpha_b Q_b^2}{R_{ab}^4})$$

$$- \frac{3}{2} f_a f_b \alpha_a \alpha_b / [(\frac{f_a \alpha_a}{n_a}) \tfrac{1}{2} + (\frac{f_b \alpha_b}{n_b}) \tfrac{1}{2}] R_{ab}^6 \qquad 2.4.1$$

$$+ \frac{g_a g_b}{R_{ab}^{12}} \}$$

or

$$\Delta E_{AB}(kJ/mole) = \sum_{a'\epsilon A} \sum_{b'\epsilon B} \{0.13894168 \times 10^4 \, Q_a Q_b / R_{ab}$$

$$-0.69470838 \times 10^3 \, (f_a \alpha_a Q_b^2 + f_b \alpha_b Q_a^2) / R_{ab}^4$$

$$-0.15160732 \times 10^4 \, f_a f_b \alpha_a \alpha_b / [(f_a \alpha_a / n_a)^{1/2}$$

$$+ (f_b \alpha_b / n_b)^{1/2}] R_{ab}^6 + 4.184 \frac{g_a g_b}{R_{ab}^{12}} \} \qquad 2.4.2$$

f_X, g_X are parameters associated with class X, with the summation now extending over the classes.

The interaction energy between atoms belonging to a particular class obtained from the expression of Clementi et al (28-30) was equated to equation 2.4.2. For values of the interatomic separation, starting at 2 Å with increments of 0.25 Å, the interaction energy calculated from equation 2.3.2.6 was fitted to equation 2.4.2. The f factor was assigned an initial value of 0.1 with increments of 0.1, and the best fit between the two expressions gives the g and

corresponding f factor (32,33) associated with the atom belonging to a particular class.

For the interactions between an ion and atoms of a certain class, the coefficients A_{ab}, B_{ab} and C_{ab} as reported (28-30) are not valid. This is mainly due to the fact that the type and magnitude of the interactions involved are different from that between two neutral molecules. Therefore, when an ion interacts with an atom, a new set of f and g factors consistent with this type of interaction have to be evaluated.

Ab-initio calculations for the interaction of Na^+ with ether, thioether and amide systems have been reported (34). Using the pair potential constants, A_{ab}, B_{ab} and C_{ab}, reported for these interactions, atoms were assigned to additional classes. The f and g factors corresponding to the new classes were calculated as described in the foregoing paragraphs.

Table 1 gives the class number and a brief description of the environment of the atom. The f and g factors along with the polarisabilities and net charge are given in Table 2

A major aim of this research was the evaluation of energy gradients for ions such as Li^+, Na^+, K^+ and Ca^{2+} during their movement through transmembrane channels. As such, it was necessary to calculate the corresponding parameters for the ions mentioned.

TABLE 1 - ASSIGNMENT OF ADDITIONAL CLASSES TO ATOMS

ATOM	CLASS	DESCRIPTION OF ATOMIC ENVIRONMENT
C	38	adjacent to $-CH_2-O-$
C	41	CH_2, adjacent to ether O
C	42	C of 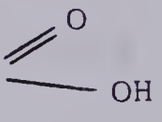
N	43	amide N
O	44	ether O
O	45	carboxylic O
H	48	CH_3, adjacent to 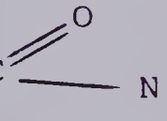
H	49	CH_3, adjacent to CH_2
H	50	CH_3, adjacent to amide N
H	53	$-CH_2$
H	56	$-CH_2$, adjacent to ether O
H	57	-amino H

TABLE 2 - PARAMETERS FOR THE NEW CLASSES OF ATOMS

ATOM	CLASS	NET CHARGE	POLARISABILITY ($Å^3$)	f	g (kcal $^{1/2}$ $Å^6$ mol $^{-1/2}$)
C	38	-.584	3.20	0.1	1492
	41	-.151	2.03	0.1	1093
	42	.421	1.30	14.2	1098
N	43	-.328	1.56	0.1	530
O	44	-.407	1.20	0.1	656
	45	-.406	1.18	0.1	655
H	48	.203	.362	27.2	561
	49	.187	.368	22.5	425
	50	.194	.365	23.4	456
	53	.195	.365	23.6	442
	56	.170	.376	19.9	383
	57	.266	.330	32.6	625

The energies of the systems $(X\text{-}X)^{n+}$, where X = Li, Na, K, n = 2; X = Ca, n = 4, were calculated as a function of the interionic distances using a standard self-consistent field technique. The basis sets used for the alkali ions were those reported in the literature (35-36). For Ca^{2+}, a basis set was generated as described below. The basis set for K^{+} (34) was scaled to the atomic charge of Calcium. With this set as the initial guess, the 17s and 11p primitive basis functions were optimised within the SCF approximation.

The method of Huzinaga et al (37) was used to generate a d polarisation function for the optimised primitive basis set. The energy of Ca^{2+} using the (17s/11p/1d)* basis set (the asterix * denotes the inclusion of the d function) was evaluated. As the interaction energy for the dicationic system was required, it was decided to contract the primitive basis set to a (9s/6p/1d)* basis to reduce the computation involved.

Table 3 gives the basis set for Ca^{2+} and the energies for the different sets considered are listed in Table 4. The parantheses in column 5 of Table 3 show the order of contraction of the (17s/11p/1d)* basis.

TABLE 3 - BASIS SET FOR Ca^{2+}

FUNCTION NO.	TYPE	ORBITAL EXPONENT	COEFFICIENT	CONTRACTED FUNCTION NO.
1	s	616081.40	0.0003989	
2	s	91024.189	0.0031309	
3	s	19819.286	0.0168379	1
4	s	5486.6766	0.0745908	
5	s	1806.0119	0.2587144	
6	s	661.37163	0.72177445	
7	s	263.20103	0.38624719	2
8	s	113.46395	0.64339195	
9	s	50.064998	0.78925512	3
10	s	21.006017	0.23416483	
11	s	9.441946	1.0	4
12	s	4.2428535	1.0	5
13	s	1.6680995	1.0	6
14	s	0.990167	1.0	7
15	s	0.64233295	1.0	8
16	s	0.33077521	0.99741795	9
17	s	0.0408167	0.005200197	
18	p	1635.0249	0.005112976	
19	p	358.18464	0.042569083	10
20	p	108.44291	0.22425999	
21	p	38.424956	0.80820775	
22	p	15.249925	0.48396169	11
23	p	6.5276260	0.56868506	
24	p	2.9077000	1.0	12
25	p	1.4962640	1.0	13
26	p	0.7307220	1.0	14
27	p	0.3547250	0.93958945	15
28	p	0.1695930	0.070519148	
29	d*	1.047	1.0	16

TABLE 4 - BASIS SETS AND THEIR ENERGIES

BASIS SET	ENERGY (a.u.)
(17s/11p)	-676.151749
(17s/11p/1d)*	-676.151753
(9s/6p/1d)* (contracted)	-676.133512
Hartree-Fock value (38)	-676.1544

Interaction energies ΔE, as a function of the distance R, for the di-ionic systems were defined as:

$$\Delta E_{(R)} = E_{X_2^{n+}(R)} - E_{X_2^{n+}(L)} \qquad 2.4.3$$

The contracted basis set was then used to calculate the energy of Ca^{2+}-Ca^{2+} for different interionic distances. where L denotes a very large inter-ionic distance, the value of which depends on the system under consideration. This definition was used so as to reduce any basis set superposition errors (39-40).

The interaction energies obtained from equation 2.4.3 are fitted to equation 2.4.2 and the corresponding parameters obtained for the best fit.

Table 5 gives the ions and their corresponding parameters.

TABLE 5 - f AND g FACTORS FOR THE IONS

ION	CLASS	f	g (kcal $^{1/2}$ Å^{6} mol $^{-1/2}$)
Li^{+}	58	11.4	37
Na^{+}	59	5.1	563
K^{+}	60	1.0	1415
Ca^{2+}	61	1.6	8644

2.5 PROGRAMMING DETAILS

The FORTRAN program used for the evaluation of the interaction energy of two systems (41) uses a Steepest-Descent method for the minimum energy search.

2.5.1 STEEPEST-DESCENT METHOD

A steepest-descent procedure of minimisation of a function F requires

(i) the selection of a starting point x_0

(ii) evaluation of the gradient vector G(0) of F at x_0

(iii) minimising the function $f = F(x_0-\lambda G_0)$, where λ is a variable step length corresponding to the largest decrease in the value of the function.

If the minimum within the desired level of convergence is not obtained, x_0 is varied as:

$$x_0 = x_0 - \lambda G_0$$

and the process repeated from step (2) above.

In the case of large systems, specially biomolecules, the potential energy contour could be composed of multiple minima. The result obtained by a steepest-descent technique could then correspond to a minimum of the contour, which may not be the global minimum.

CHAPTER 3 - RESULTS OF THE CALCULATIONS

The intracellular medium of a neuron has a higher concentration of K^+ compared to its exterior, while Na^+ are found in larger concentrations outside the cell. As discussed in Chapter 1, the transport of these ions through the Sodium channel and the consequent changes in the ratio of their intracellular to extracellular concentrations is responsible for the action potential. This action potential, propagated along the nerve axon, is primarily responsible for the release of the neurotransmitters into the synaptic cleft. Thus, the permeability of the Sodium channel to ions is important in understanding the mechanisms of nervous transmission.

As the structure of the Sodium channel is still to be elucidated, suitable models have to be used in order to study its interactions with ions. The choice of the model is based on the experimental information available. It has been found (42) that ions having a diameter larger than 5 Å hardly penetrate the channel and, furthermore, that a decrease in the pH significantly reduces the conductance of the ions through the channel. The latter observation suggests that in its active form, the Sodium channel has negatively charged carboxylate groups. These groups can then be thought of as an effective coordination sphere which facilitates the passage of the cations.

Antibiotics synthesised by microorganisms make membranes permeable to certain ions. The linear polypeptide Gramicidin-A is an example of such a transmembrane antibiotic which specifically facilitates the diffusion of monovalent cations (43-46). It consists of fifteen amino acid residues arranged in the following sequence:

HCO-L-Val-Gly-L-Ala-D-Leu-L-Ala-D-Val-L-Val-D-Val-L-Trp-D-Leu-L-Trp-D-Leu-L-Trp-D-Leu-L-Trp-$NHCH_2CH_2OH$.

The transmembrane ionophore is a dimer of Gramicidin-A and forms a channel through which the ions can diffuse (47-51).

Four models were postulated for the structures of the dimer. Urry et al (50-53) suggested the N-terminal to N-terminal structure while the C-terminal to C-terminal model was preferred by Bradley et al (54). An anti-parallel double helix structure (55) based on conformational studies on Gramicidin-A in non-polar organic solvents (56) and a parallel-β double helix with both N-termini at one end have also been proposed. Nuclear magnetic resonance studies on the Gramicidin-A dimer in phosphatidylcholine vesicles (57) shows a strong N-terminal to N-terminal binding favouring the first model as the major conformation of this transmembrane antibiotic. Further studies (58) showed that the carbonyl groups of the dimer are directed towards the channel axis and the diameter of the channel is about 4 Å in

the absence of ion occupancy. Thus, the polypeptide and structural nature of the Gramicidin-A dimer makes it a suitable model for studying the Sodium channel.

The results presented in this chapter were obtained by the application of the method described in section 2.4 to the interaction of ions and molecules with a theoretically generated structure for the dimer.

3.1 GENERATION OF A STRUCTURE FOR THE GRAMICIDIN-A DIMER

Two methods were used to obtain the atomic coordinates of the ionophore. The method of Scheraga et al. outlined in section 2.3.1 was used in both cases to calculate the configuration of the polypeptide sequence.

The computer program based on this method (59) does not allow for a $-NH\cdot CH_2\cdot CH_2\cdot OH$ end group. Therefore, for computational purposes, this entity was replaced by $-NH\cdot CH_3$. The first method, referred to as the 'segmented approach' is described below.

The fifteen amino acid polypeptide chain was divided into three consecutive segments of five residues each. Values for the dihedral angles, except for that about the peptide bond, for each of the amino acids were taken from the literature (60-61). The energy of each segment was calculated as a function of the diheral angles between each pair of amino acids. For each calculation, these angles

were varied, in turn, by increments of 7.5°. Using this strategy, the conformation of each segment corresponding to its lowest energy was determined.

In order to obtain the geometry of the entire molecule, the optimised segments were linked sequentially. The energetically favourable orientation of the linkage between the pairs of segments was decided by calculating the energy of the linked segment as a function of the new dihedral angle formed during the joining of the segments. The structure of the Gramicidin-A molecule, obtained using the above strategy, was plotted on a Tektronix T-4015 terminal adapted with a hard copier. The plot obtained was that of a globular protein and not a channel, indicating that the strategy described above was a failure in this particular application.

In the second method, dihedral angles for the backbone of polypeptide helices were used to generate a possible structure for Gramicidin-A. Three helices were chosen (62) namely (i) the L-D Alanine helix, (ii) the L-D Valine helix and (iii) a hypothetical helix in which the L-D Ala helical angles were used for the Gly and Ala residues, the L-D Val angles for Leu and Val residues and the L-D Phe angles for the Trp residues. The side chain dihedral angles were not optimised during the calculation of the conformation of each of the helices described above. Table 6 gives the energy corresponding to each conformation.

Table 6 CHOICE OF HELIX FOR THE BACKBONE OF GRAMICIDIN-A AND THE CORRESPONDING ENERGY.

CHOICE OF HELIX	ENERGY (kJ/mole)
L-D Ala	8616
L-D Val	23390
L-D Ala + L-D Val + L-D Phe	very large

As the energy calculated for the conformation generated with the first choice of angles was the lowest, this structure for Gramicidin-A was used for all the calculations reported in this thesis.

Figures 1 and 2 are the side and front views of the Gramicidin-A molecules. In the second picture the carbonyl and amino groups of the peptide bond point towards the axis of the channel.

The dimer of Gramicidin-A, which was used as a model for the Sodium channel, is formed from two such monomers. The distance, between the N termini of these moieties which face each other, was varied until a minimum in the energy of interaction between the monomers was obtained. At this point, the second molecule was rotated about the channel

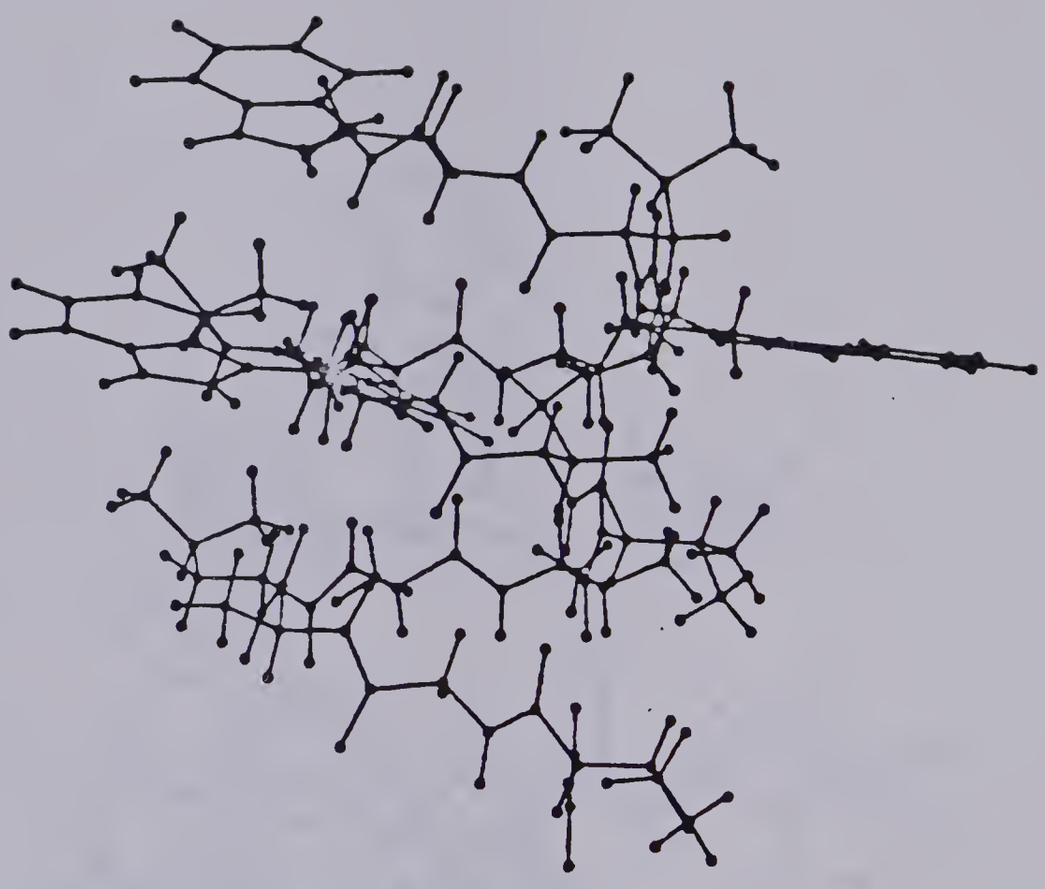

FIGURE 1 - SIDE VIEW OF THE GRAMICIDIN-A MOLECULE.

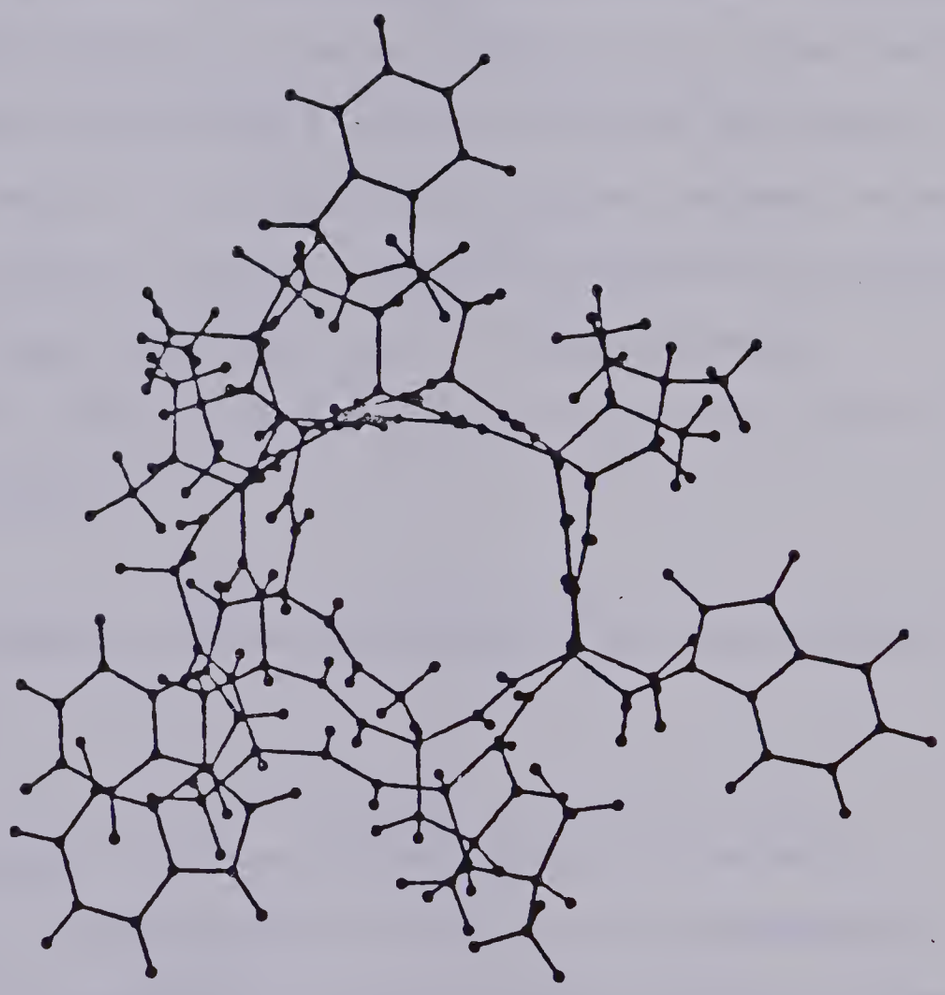

FIGURE 2 - FRONT VIEW OF THE GRAMICIDIN-A MOLECULE.

axis relative to the first. The angle at which a minimum interaction energy was obtained was taken as that which best described the position of the second molecule in the dimer. The distance between the N-termini of the monomers was calculated to be 2.5 Å, which makes the overall length of the dimer 29.5 Å. This value is in excellent agreement with the experimentally observed value of 30 Å when embedded in a membrane (63) and 32 Å when in methanol or ethanol (64). The angle of rotation of the second monomer relative to the first was 0° and the energy of interaction between the monomers was calculated to be -126.66 kJ/mole.

Figures 3 and 4 show the lateral and front views of the entire ionophore.

3.2 IONIC MOVEMENT THROUGH THE PORE OF THE TRANSMEMBRANE CHANNEL

At present, the Gramicidin-A dimer is the only structurally characterised ion selective transmembrane channel. It is permeable to monovalent cations but does not allow the passage of dications or anions (46). Conductance measurements for the transport of some of the monovalent cations (65) gave the following order for their permeability ratios (given in parenthesis) with respect to Na^+:

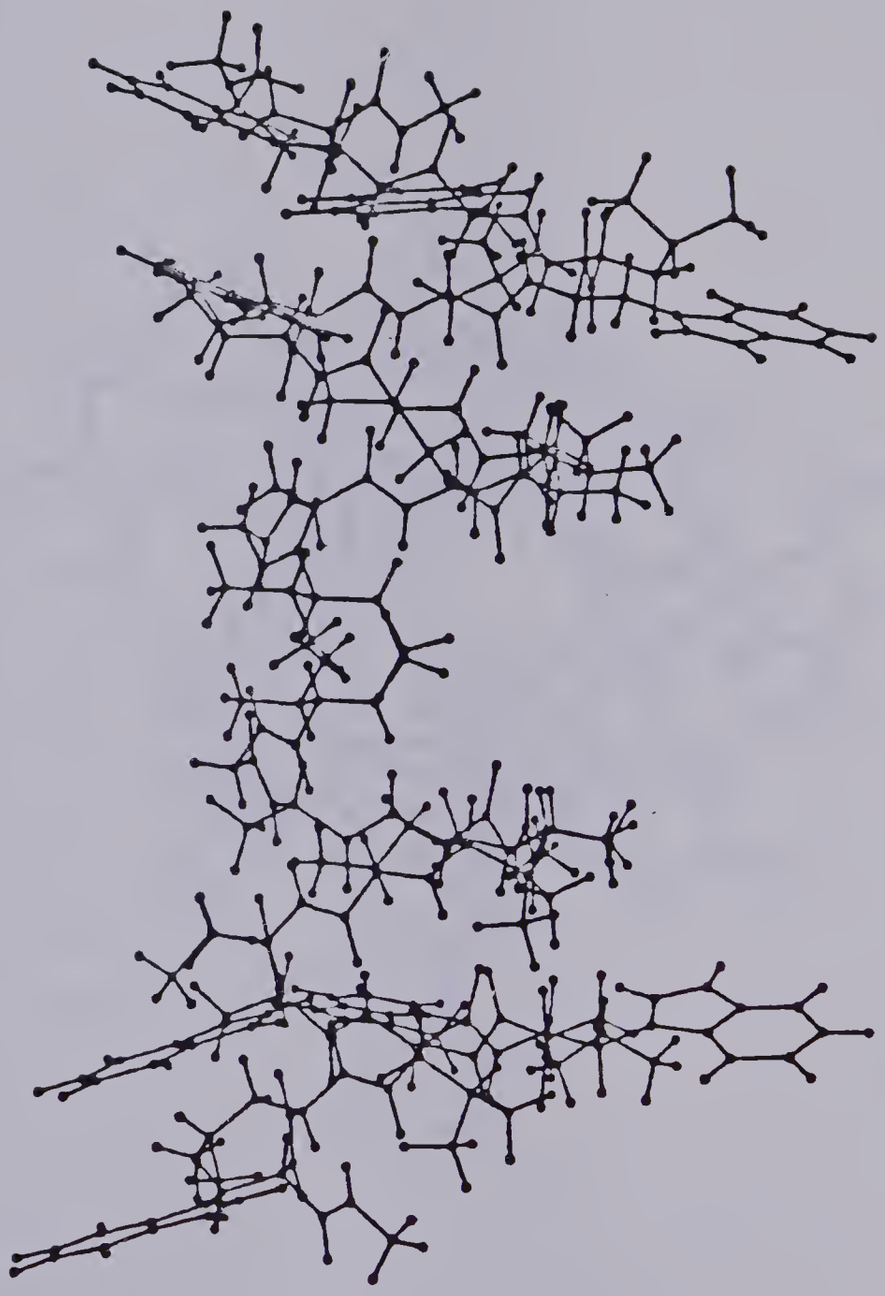

FIGURE 3 - LATERAL VIEW OF THE GRAMICIDIN-A DIMER.

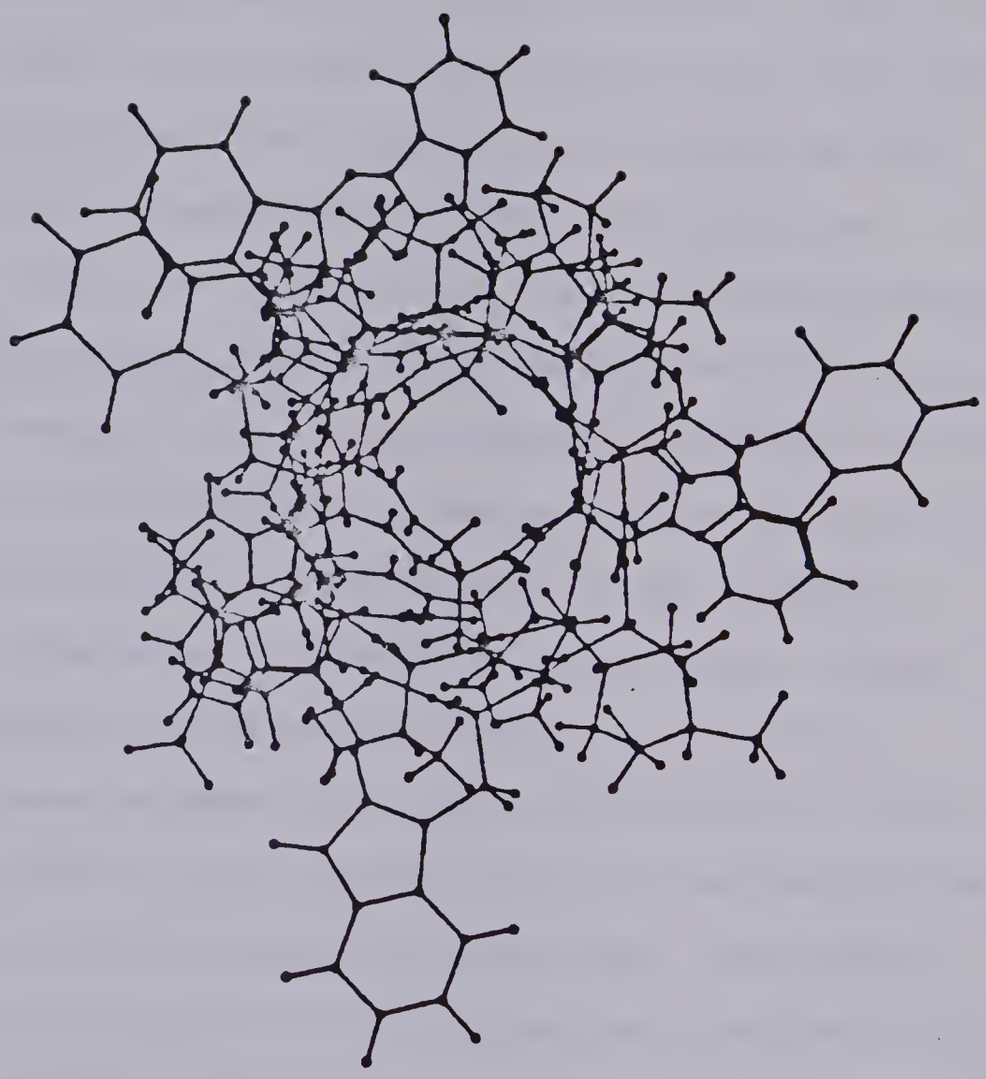

FIGURE 4 - FRONT VIEW OF THE GRAMICIDIN-A DIMER.

H^+ (150) > NH_4^+ (8.9) > Cs^+ (5.8) > Rb^+ (5.5) > K^+ (3.9) Na^+ (1.0) > Li^+ (.33)

As the diameter of the channel is about 4 Å, a fully hydrated ion will not be able to pass through. Thus, it is a partially hydrated ion that moves through the pore with its vacant hydration sites directly coordinated by the peptide moieties, namely the carbonyl grups, of the ionophore. Effective coordination may require conformation changes in the polypeptide and this mechanism is known as librational motion (66). A consequence of peptide libration is a change in the length and diameter of the channel. As the coordinating group in the peptide is the carbonyl chromophore, the negative charge on the carbonyl oxygen makes the channel selective for cations over anions.

It has been proposed (58) that the proximity of the surrounding lipid is an essential factor in explaining the impermeability of the channel to dications. The single coordination layer provided by the peptide moieties in the backbone of the Gramicidin-A dimer is not sufficient to shield the divalent cation from the lipid around the channel.

The selectivity among the monovalent cations can be explained on the basis of their ionic radii. In Table 7, the ionic radii for the cations studied are listed.

Table 7 IONIC RADII

ION	RADIUS (Å)
Li^+	0.68
Na^+	0.98
K^+	1.33
Ca^{2+}	0.99

The transport of the smaller ions (e.g., Li^+) will require greater coordination by the carbonyl groups and the energetics of the associated changes in the conformation of the polypeptide will make the process less favourable. Hence the low permeability ratio for Li^+.

The free energy profile for the transport of Na^+ through the malonyl gramicidin channel has been determined using Sodium-23 NMR (67-69). Two binding sites, one in each monomer, separated by a distance of 20 Å and a central energy barrier between these sites were observed. Clearly, the value of this central energy barrier will bear a direct relationship to the ease of passage of the ion through the ionophore; the larger the value, the more difficult it will be for the ion to move through the channel. Extending this argument, the energy barrier for the dications should be much larger than that for the alkali ions.

Using the method of calculation described in section 2.4 the movement of an ion X (X = Li^+, Na^+, K^+, Ca^{2+}) through the modified Gramicidin-A dimer was studied. The new classes, for the interaction of atoms with ions (Table 2), and the corresponding parameters were used for those atoms comprising the backbone of the polypeptide chain.

For each of the ions studied, the energy profile was consistent with the experimentally observed two-site binding theory with a central energy barrier.

In Table 8, the central energy barrier E_c (kJ/mole) and the distance d (in Å) separating the binding sites are given. It must be emphasised that in all the calculations and results described in this chapter, the librational mechanism of the polypeptide chain has not been included.

Table 8 E_c AND d FOR TRANSPORT THROUGH THE GRAMICIDIN-A DIMER

ION	E_c (kJ/mole)	d(Å)
Li^+	218	14
Na^+	121	12
K^+	209	12
Ca^{2+}	318	13

Based on the values of E_c, the calculated order of permeability for the ions was:

$$Na^+ > K^+ > Li^+ > Ca^{2+}$$

which is not consistent with the experimental observations given above. Besides, this model for the ionophore allows Ca^{2+} to move through the channel when in fact it is found to be a channel poison blocking it, just inside the opening. Figures 5, 6, 7 and 8 show the path, taken by Li^+, Na^+, K^+ and Ca^{2+}, respectively.

The environment of the ionophore was modified by simulating the lipid bilayer. Initially, only the polar head group of the lipid molecule was considered. Formic acid was chosen for this purpose and its geometry obtained from X-ray data (70).

Twelve molecules of formic acid were placed, one at a time, around the mouth of a Gramicidin-A molecule. The position of the n-th formic acid molecule is that one corresponding to the lowest interaction energy with the Gramicidin-A and the (n-1) formic acid molecules already present. Figure 9 is a plot of Gramicidin-A with the surrounding molecules of formic acid and in figure 10 only the formic acid molecules are shown for clarity. The dimer of the modified channel was obtained in the same manner as for the Gramicidin-A dimer. The energy of interaction

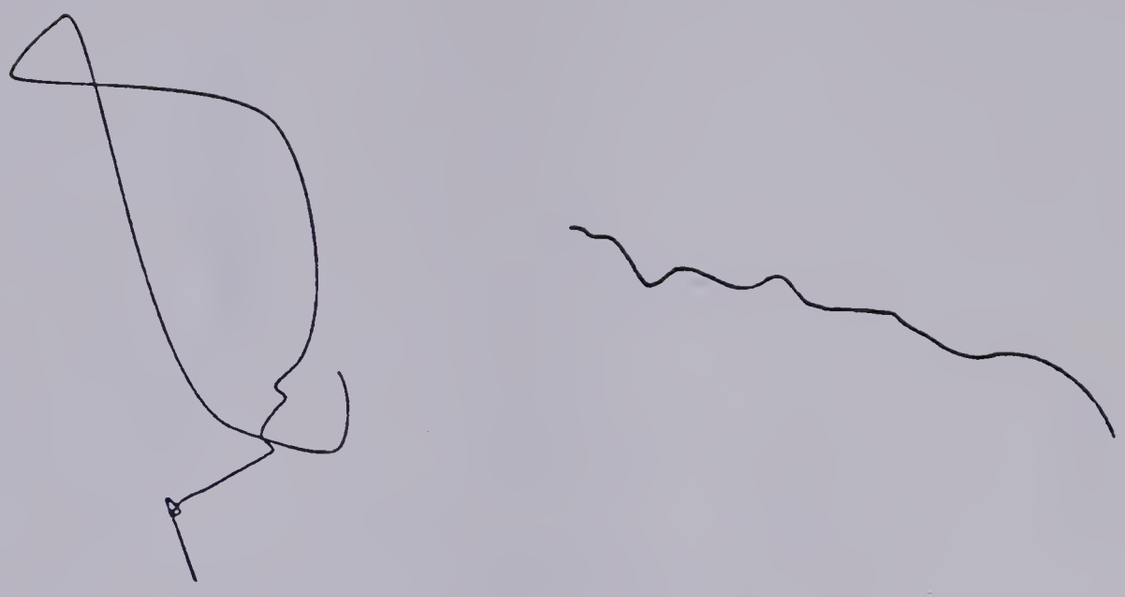

FIGURE 5 - FRONT AND LATERAL VIEW OF PATH TAKEN BY Li^+.

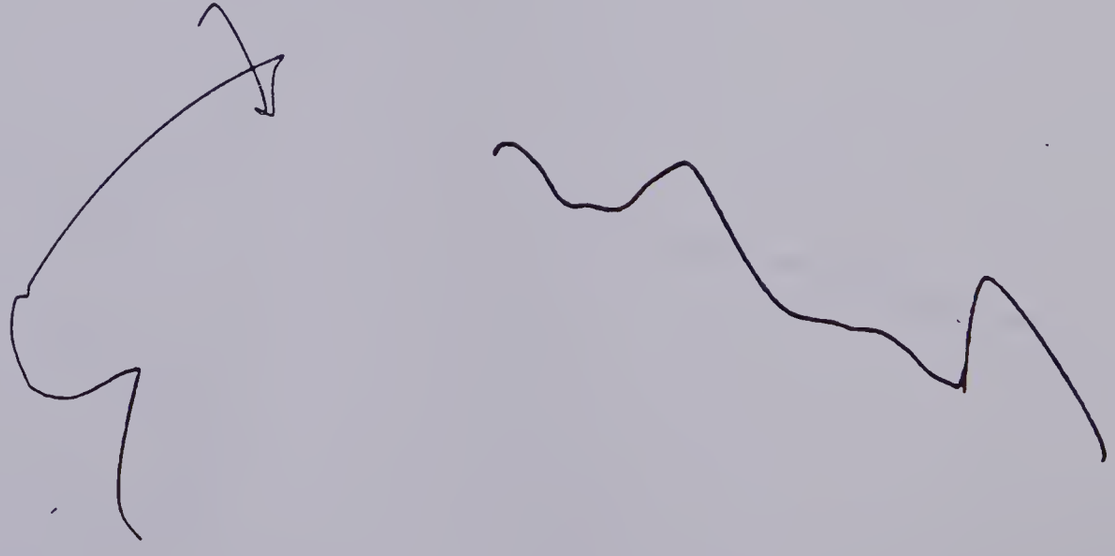

FIGURE 6 - FRONT AND LATERAL VIEW OF PATH TAKEN BY Na^+.

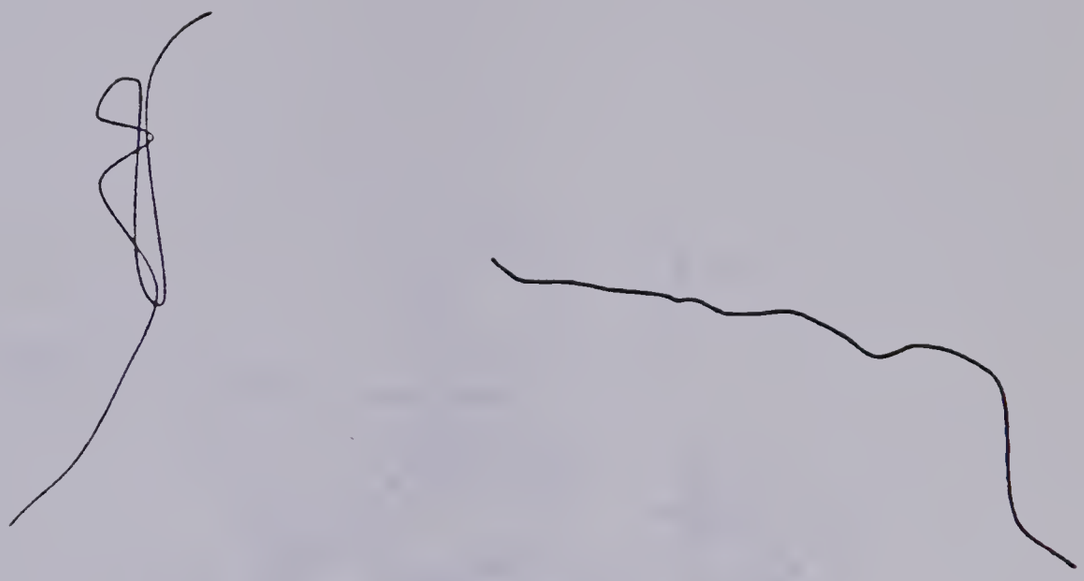

FIGURE 7 - FRONT AND LATERAL VIEW OF PATH TAKEN BY K^{+}.

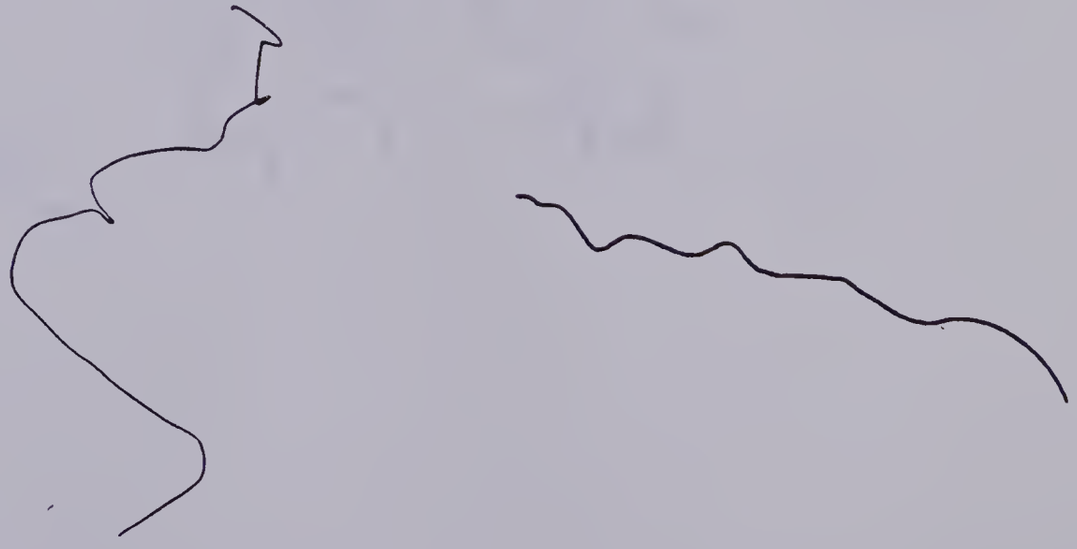

FIGURE 8 - FRONT AND LATERAL VIEW OF PATH TAKEN BY Ca^{2+}.

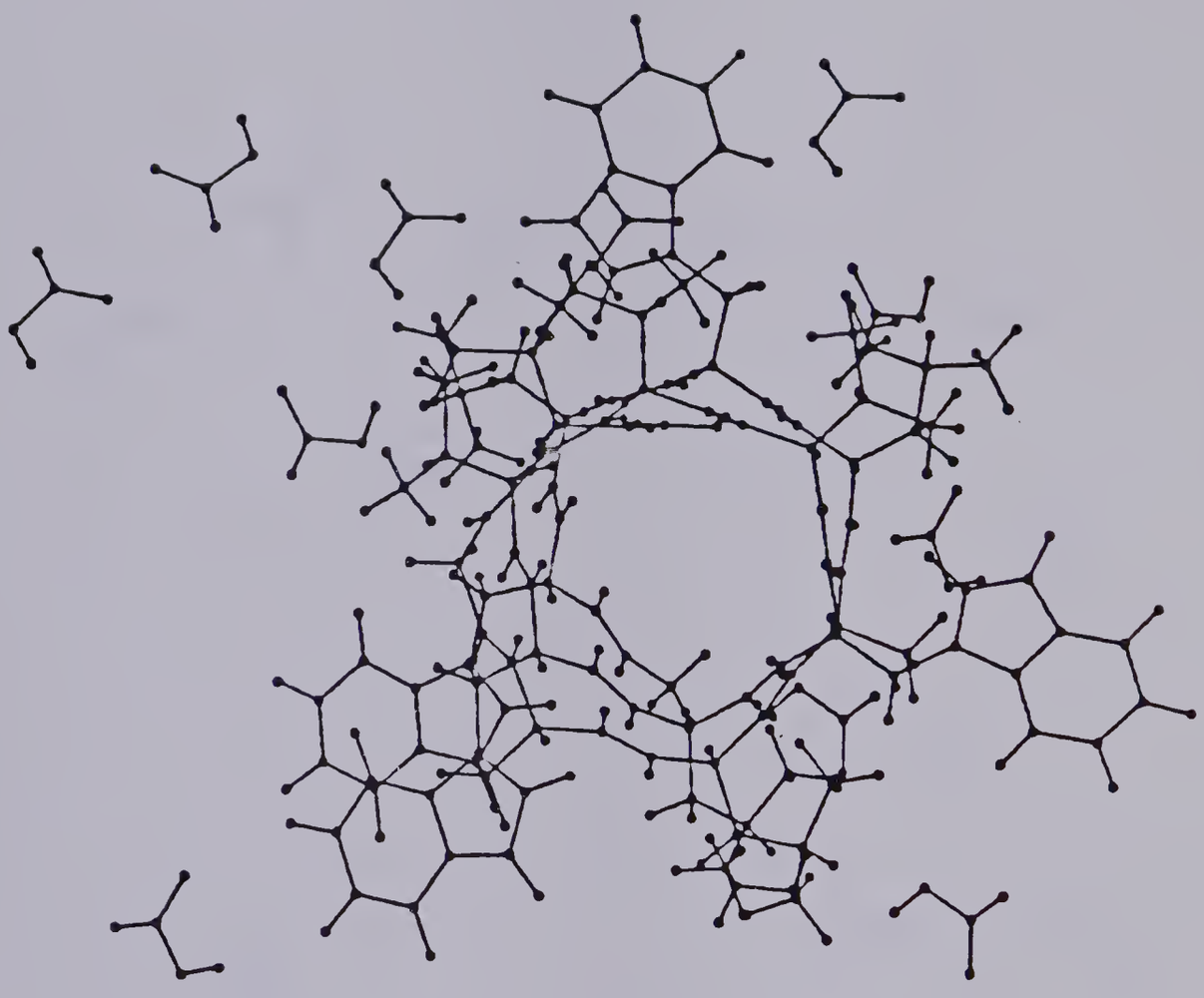

FIGURE 9 - FRONT VIEW OF GRAMICIDIN-A WITH FORMIC ACID MOLECULES.

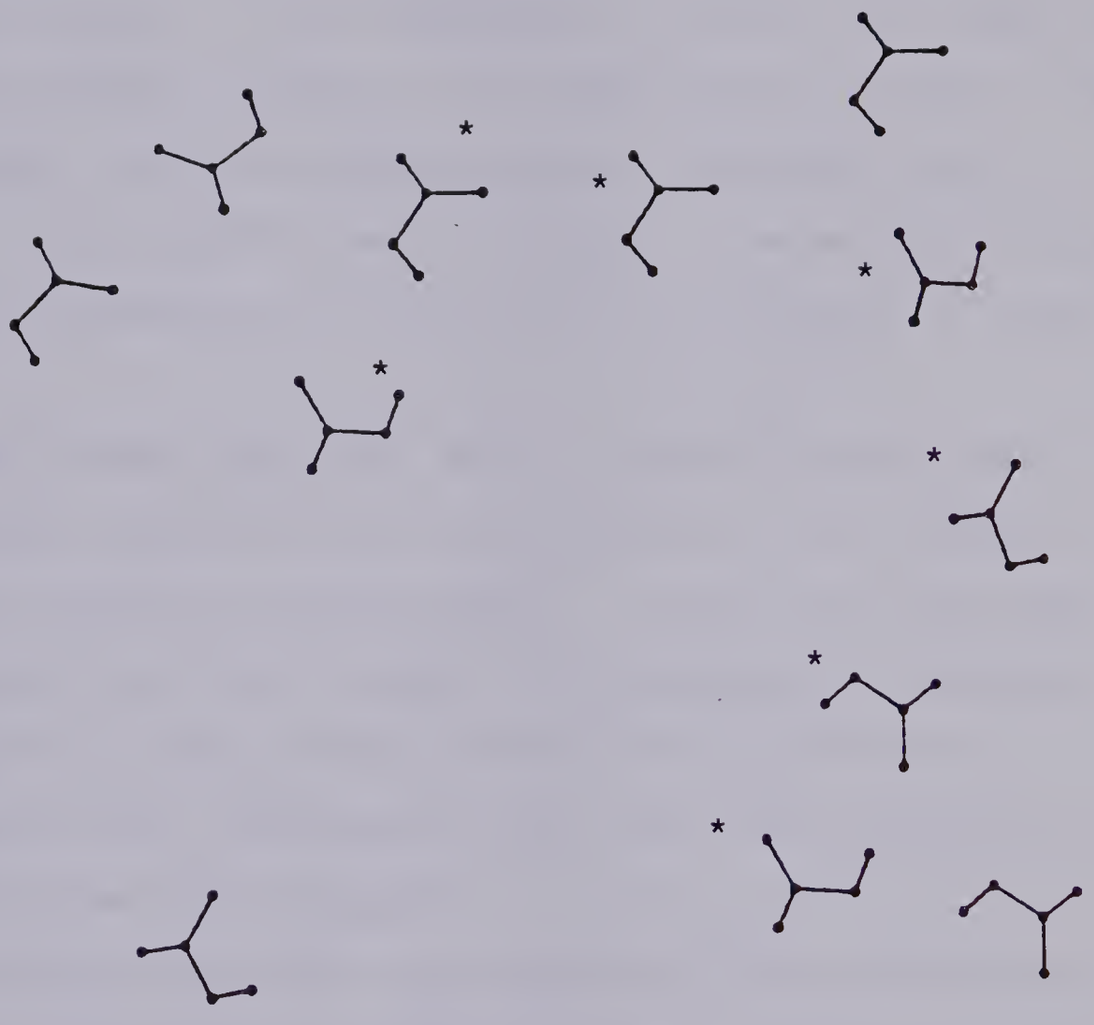

FIGURE 10 - CLUSTER OF FORMIC ACID MOLECULES AROUND THE PORE.

between the monomers was -127.16 kJ/mole. The lateral and front views of the entire modified dimer are shown in figures 11 and 12, respectively.

In order to study the transport of ions through the modified channel, it was necessary to reassign the atoms in the acid molecules closer to the mouth of the channel to the new classes. This was done in order to take the ionic nature of the interactions into accout. The molecules whose atoms were reassigned are indicated by an asterix in figure 10.

Each of the ions, Li^+, Na^+, K^+ and Ca^{2+} were placed just inside the pore of the modified channel and allowed to find their paths of minimum energy. In each case the ions were pushed out of the channel. This showed the existence of a positive energy gradient which the ions could not overcome and the inadequacy of the formic acid molecules in describing the lipid bilayer.

A further refinement was carried out by placing four molecules of octane per modified monomer, under the network of acid molecules so as to simulate a lipid environment around the polypeptide chain. The result for a monomer is shown in figure 13. Figure 14 shows the pore of the monomer in the refined model.

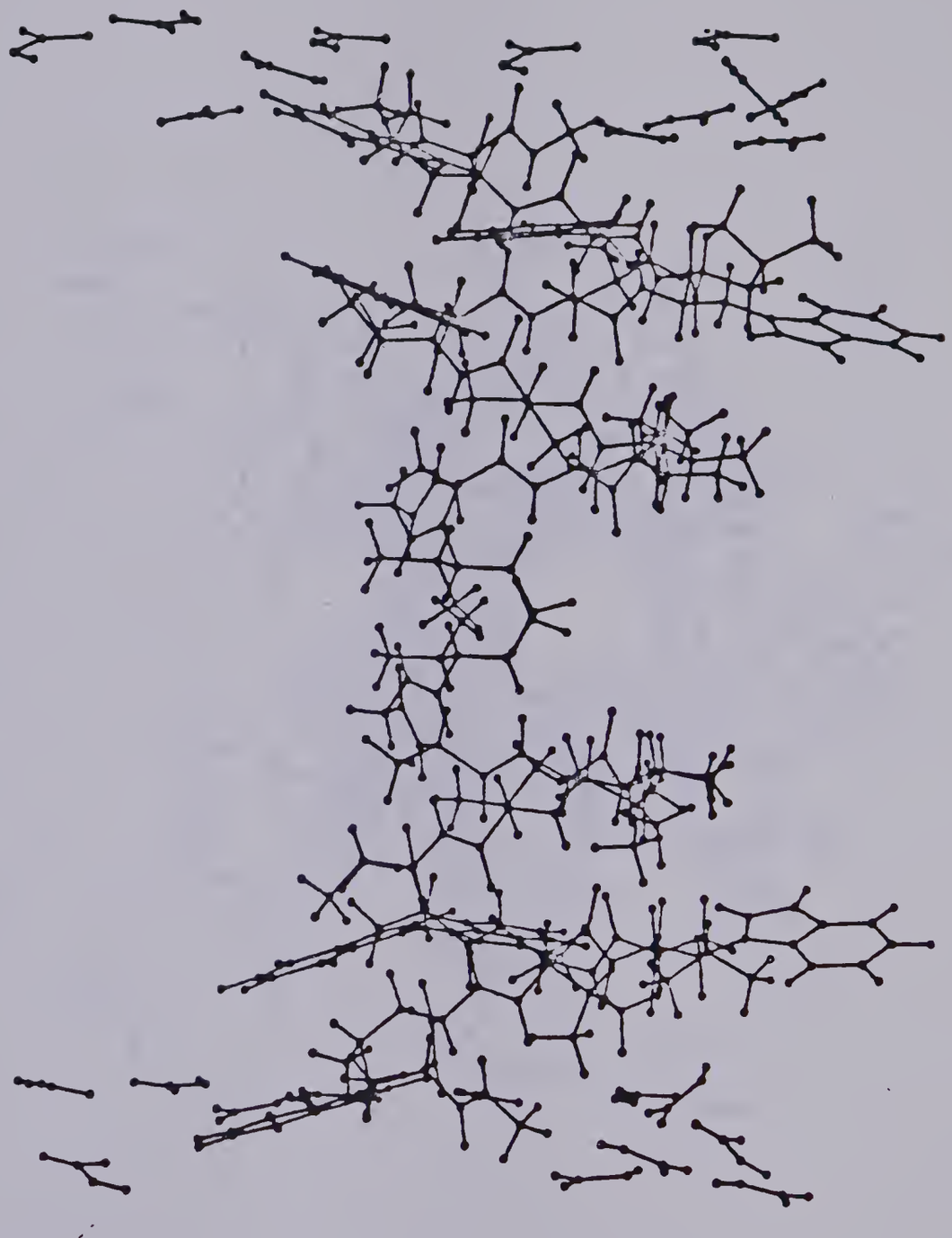

FIGURE 11 - LATERAL VIEW OF THE GRAMICIDIN-A DIMER WITH THE SURROUNDING MOLECULES OF FORMIC ACID.

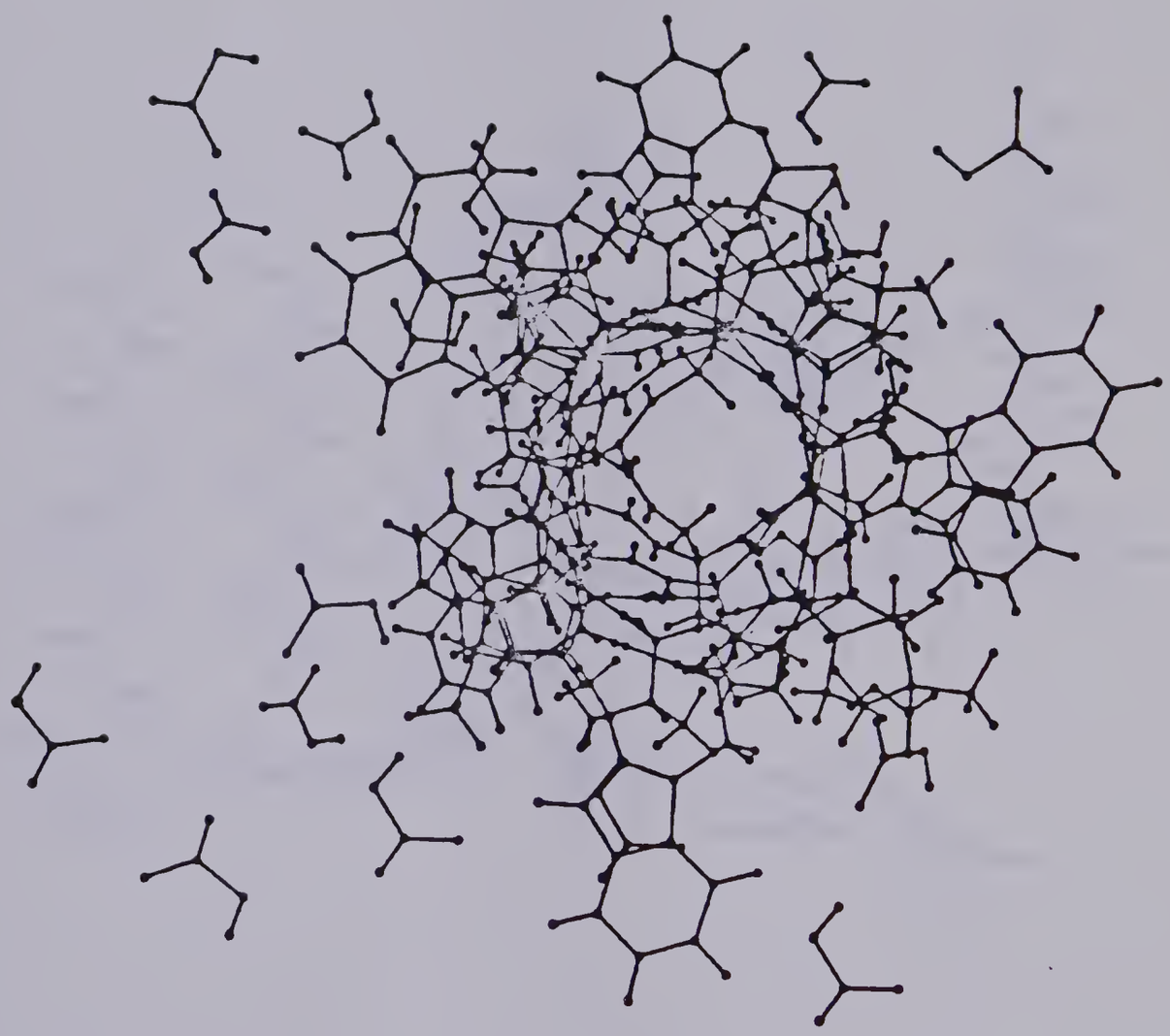

FIGURE 12 - FRONT VIEW OF THE GRAMICIDIN-A DIMER WITH THE SURROUNDING MOLECULES OF FORMIC ACID.

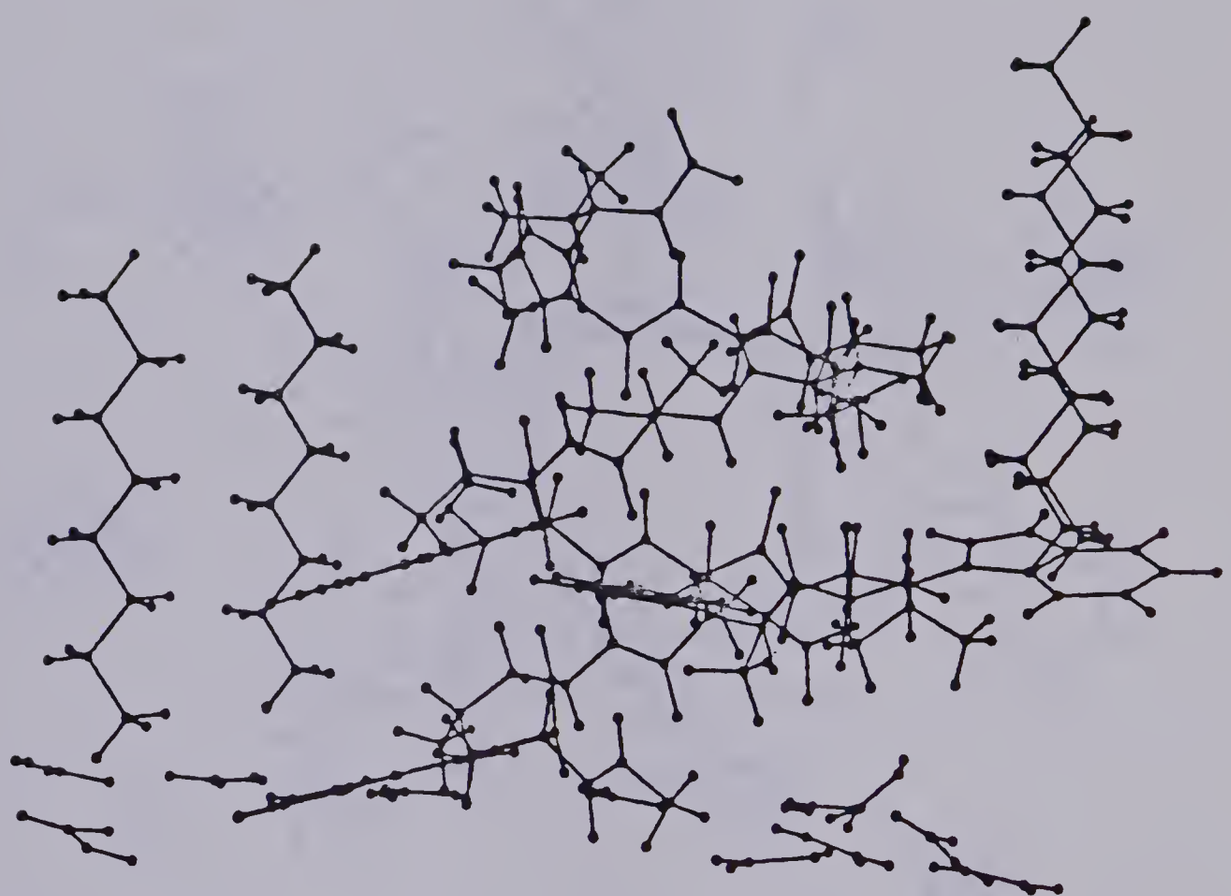

FIGURE 13 - SIDE VIEW OF THE REFINED MODEL OF A GRAMICIDIN-A MONOMER.

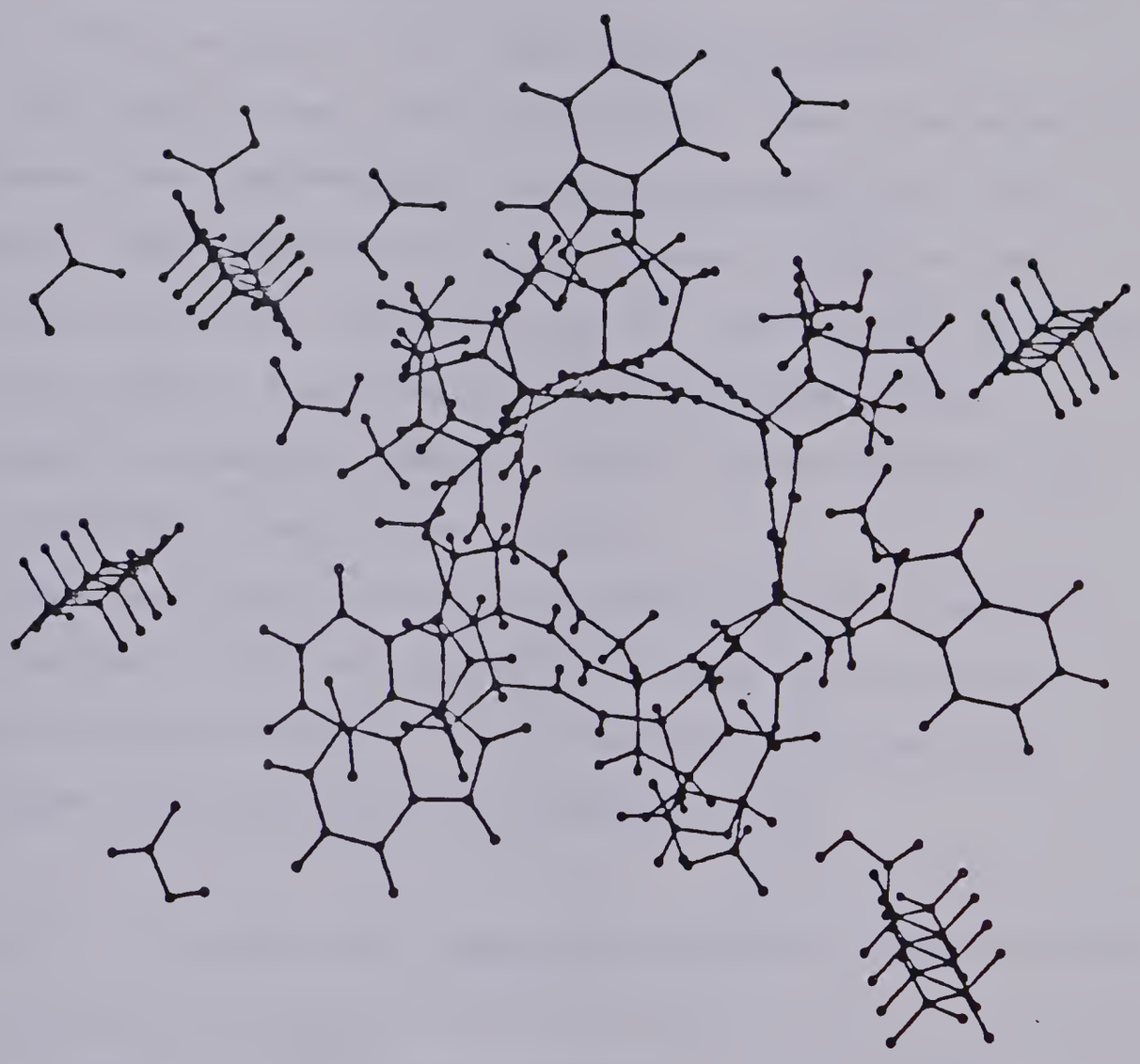

FIGURE 14 - THE PORE OF THE REFINED MODEL FOR GRAMICIDIN-A.

As proposed by Urry et al. (71), a compressing of the lipid layer at the site of the transmembrane channel was included by moving the entire simulated lipid environment (i.e., formic acid and octane molecules) by a distance of 1.5 Å. This value of 1.5 Å was chosen arbitrarily.

The dimer of two such molecules was then considered to represent the transmembrane channel, embedded in a lipid bilayer. The interaction energy between the halves was evaluated using the same strategy for dimerisation as in the previous cases. The value of the interaction energy obtained was -145.67 kJ/mole. Figures 15 and 16 show the side and front views of the channel.

The ions under consideration were allowed to move in the ionophore under the potential created by the dimer. Table 9 gives the central energy barriers (E_c) and the distances (d) between the two binding sites.

Table 9 E_c AND d FOR TRANSPORT THROUGH THE REFINED MODEL

ION	E_c (kJ/mole)	d (Å)
Li^+	265	12
Na^+	140	11
K^+	132	12
Ca^{2+}	very large	

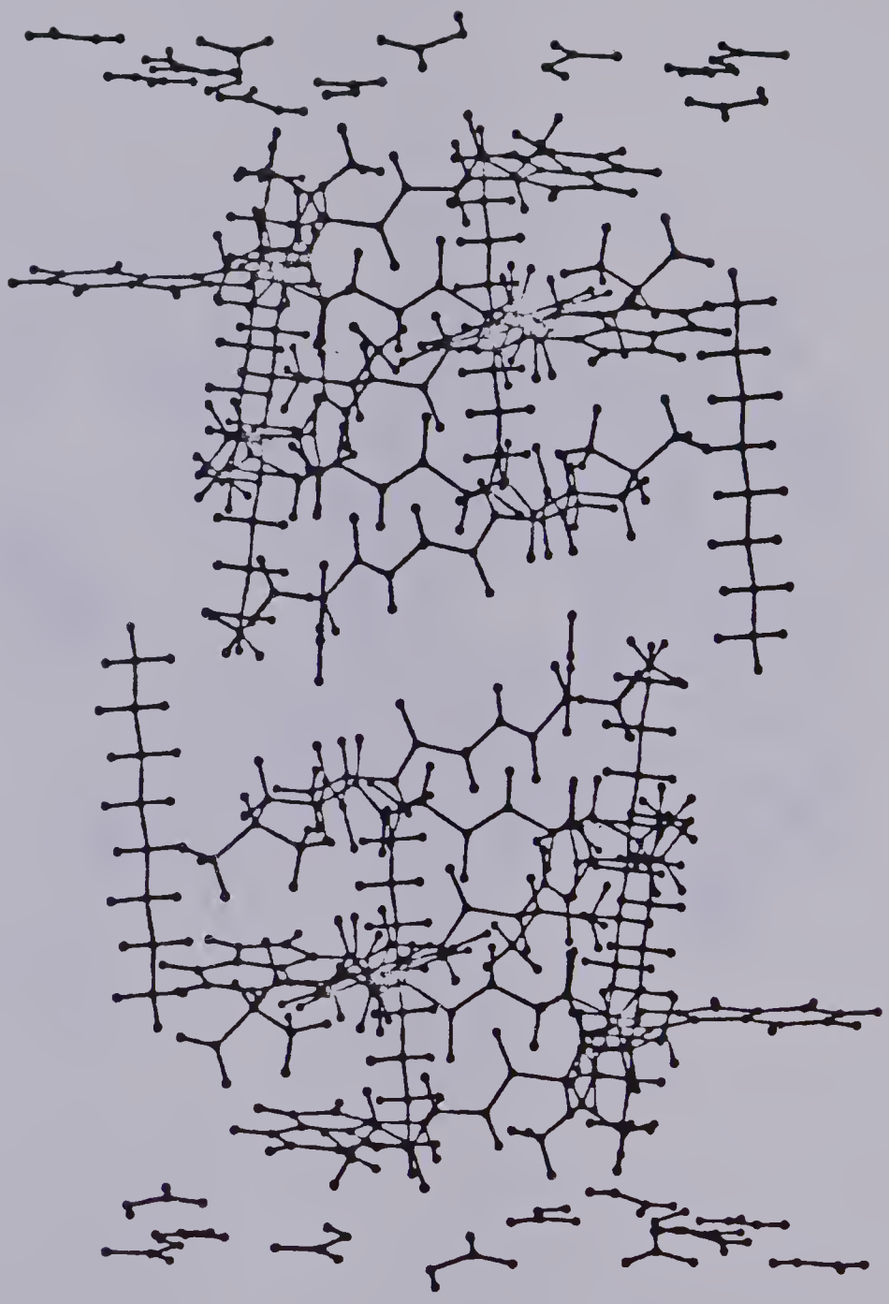

FIGURE 15 - SIDE VIEW OF THE REFINED CHANNEL.

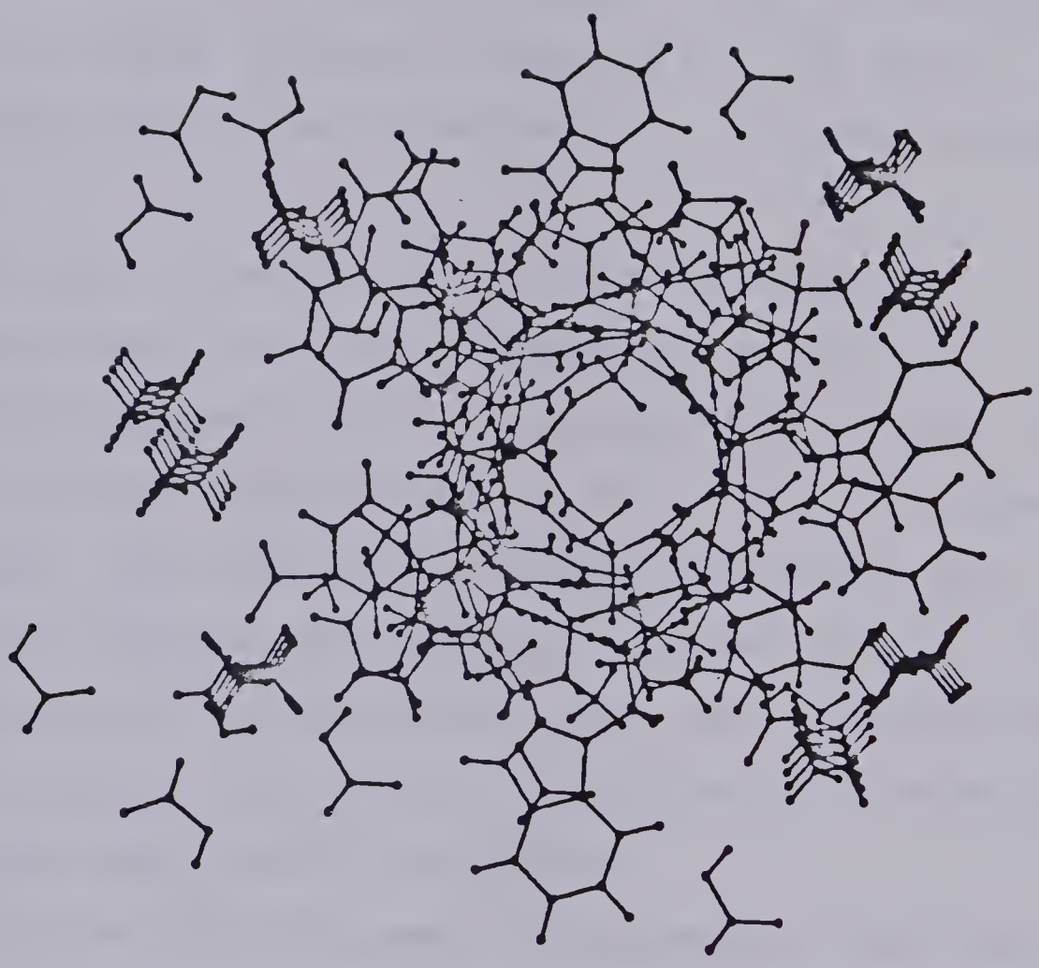

FIGUPE 16 - FRONT VIEW OF THE REFINED CHANNEL.

The predicted order of permeability is $K^+ > Na^+ > Li^+ >>> Ca^{2+}$ in excellent agreement with experiment. The channel poisoning nature of Ca^{2+} is amply illustrated by the very high energy of interaction ($.29 \times 10^6$ kJ/mole) at a distance of about 1.5 Å from the pore, inside the channel. Figures 17, 18 and 19 show the path of Li^+, Na^+ and K^+ through the pore of the refined model for the transmembrane channel.

The final refinement to the model consisted of including a chain of water molecules in the pore, as observed by Finkelstein (72). Six molecules of water, three in each monomer, were arranged one at a time in the pore of the channel. The first water molecule was placed just outside the mouth of the channel at the position which gave the lowest energy of interaction. The same criterion was used in arranging the others, the sixth molecule being just outside the other end of the channel.

As in the previous cases, the movement of the ions through the solvated pore was determined and the central energy barriers (E_c) and distance of separation (d) of the binding sites evaluated. The corresponding values are listed in Table 10.

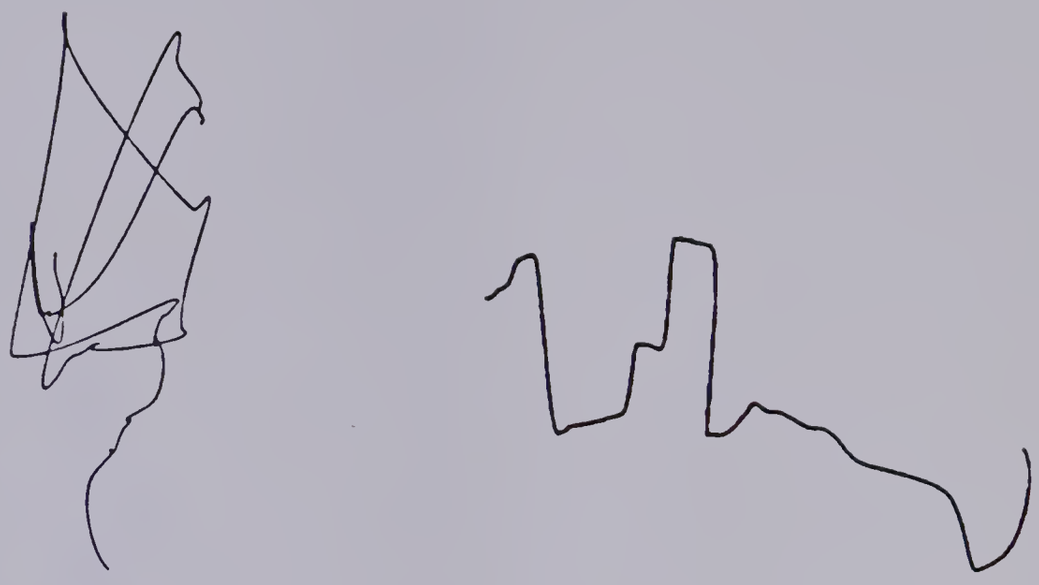

FIGURE 17 - FRONT AND LATERAL VIEW OF THE PATH OF Li^+ THROUGH THE PORE OF THE REFINED MODEL.

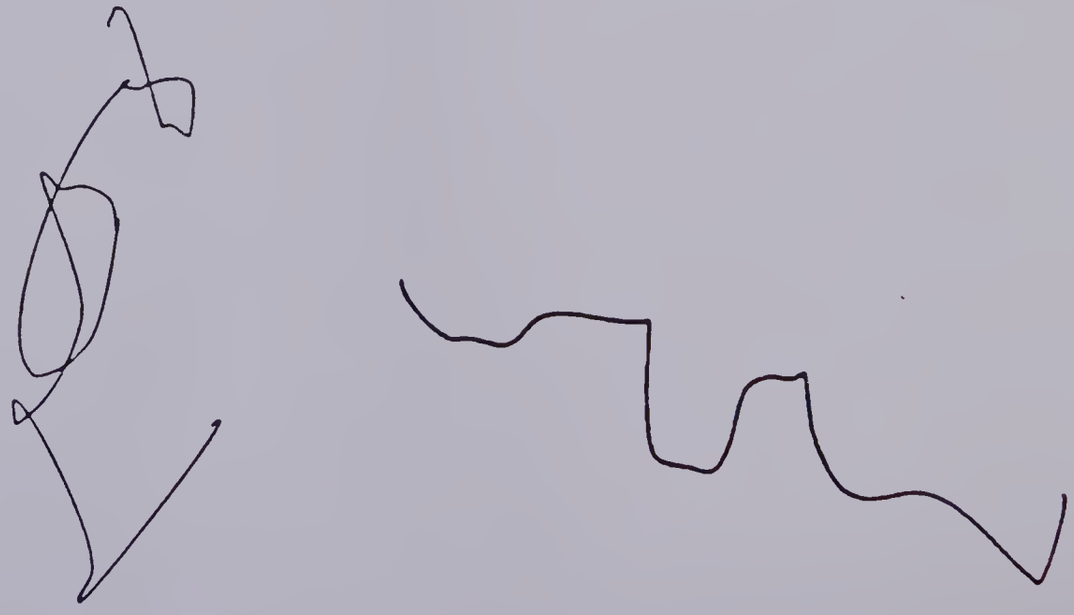

FIGURE 18 - FRONT AND LATERAL VIEW OF THE PATH OF Na^+ THROUGH THE PORE OF THE REFINED MODEL.

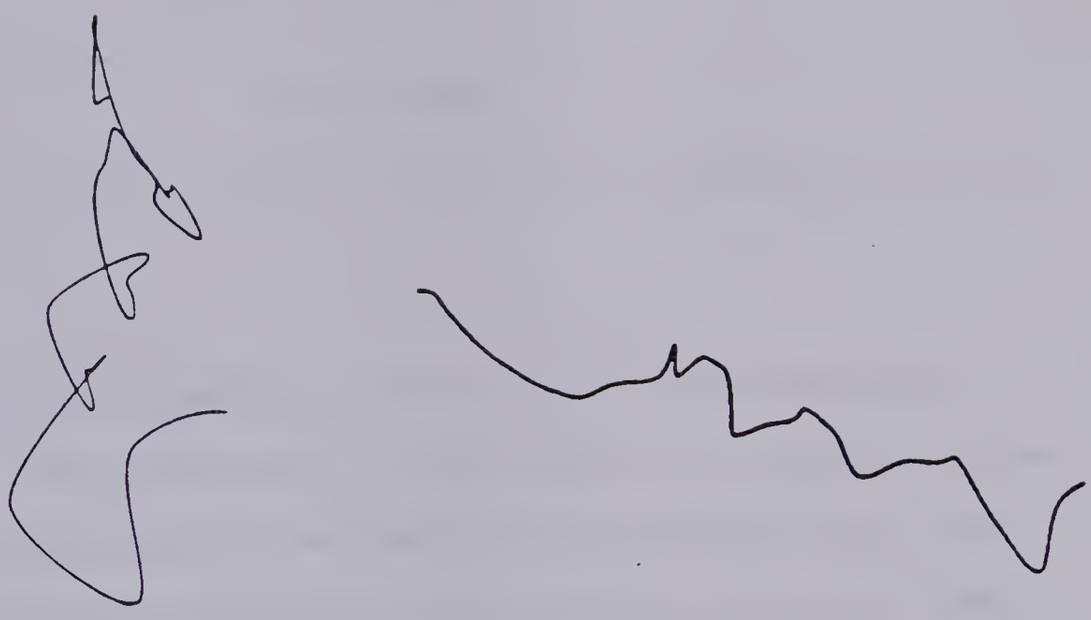

FIGURE 19 - FRONT AND LATERAL VIEW OF THE PATH OF K^+ THROUGH THE PORE OF THE REFINED MODEL.

TABLE 10 E_c AND d FOR TRANSPORT THROUGH THE SOLVATED PORE.

ION	E_c (kJ/mole)	d (Å)
Li^+	222	13
Na^+	121	12
K^+		
Ca^{2+}	very large	

The channel poisoning nature of Ca^{2+} is shown again in this model. The improvement to the model by including water molecules in the pore is demonstrated by the fact that the passage of K^+ is hindered. In other words, with the fixed conformation for the polypeptide chain and simulated lipid and hydration environment, the potassium ion does not pass through the pore. This observation is an indication of the importance of peptide libration in ionic transport. Koeppe et al. (73) have reported that the binding of K^+ to the channel widens the channel diameter to 6.8 Å while shortening its length from 32 Å to 26 Å.

The results presented in this section illustrate the improvements to the model of the transmembrane channel according to their manifestations on the transport parameters E_c and d. With each stage of improvement, the

agreement between the calculated and experimental permeability trends was better. However, the distance separating the binding sites was not comparable with the experimental value of 20 Å obtained for Na^+ (67-69).

The spiral nature of the movement of the ions when viewed along the channel axis (Figures 5-8, 17-19), indicate that the ions coordinate with the carbonyl groups during transport. This observation shows that peptide libration should be considered in any further improvements to the simulation of ionic transport.

3.3 INTERACTION OF THE CHANNEL WITH MOLECULES

In the preceeding section, a model for the transmembrane channel embedded in a lipid was refined in stages and the transport properties of certain ions through the pore of this channel studied. As discussed in section 3.2, the last refinement, which included a chain of water molecules through the pore, best described the energy profiles for the movement of these ions. It is this final model which is used to study interactions between the channel and certain molecules of biological interest.

The importance of ionic transport in initiating the action potentials has been discussed in the first chapter of this thesis. Interference with the transport of an ion affects its concentration ratio within and outside the

cell. This has a direct influence on the action potential which in turn effects the release of neurotransmitters into the synaptic cleft. Thus, a molecule which hinders the passage of ions through the pore by blocking the channel will inhibit nervous transmission. That is, a neurotoxin can be thought of as a molecule which, being strongly attached to the mouth of the channel effectively blocks the pore restricting the migration of ions through the transmembrane channel.

On the other hand, a molecule which interacts weakly with the channel would have a temporary inhibitory effect on the release of neurotransmitters. Thus, the interaction between molecules which induce general anesthesia and the channel pore can be considered to be weak. In addition, the blocking of the channel pore by such molecules needs not interrupt completely the ionic transport.

3.3.1 TOXICITY OF TETRODOTOXIN AND SAXITOXIN

The marine toxins, tetrodotoxin and saxitoxin (Figure 20), have been known to block the conduction of nerve impulses along an axon.

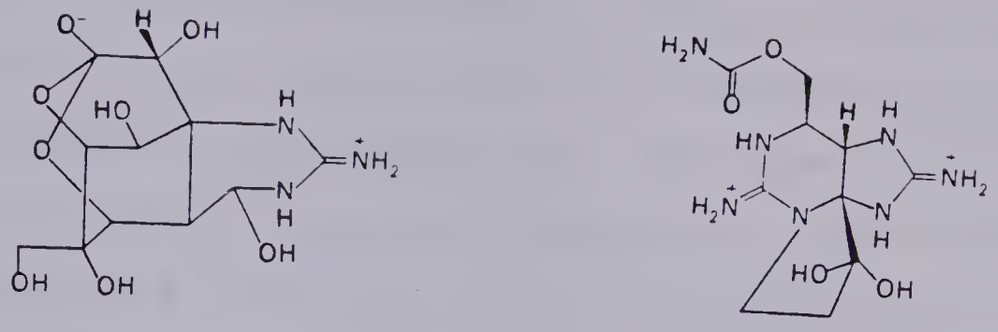

FIGURE 20. STRUCTURES OF TETRODOTOXIN (LEFT) AND SAXITOXIN (RIGHT).

Their toxic nature has been related to the very strong binding to the Sodium channel and the common structural entity, the guanidinium ion, associated with this channel blocking character (42,74). This hypothesis assumes that the guanidinium ion behaves like Na^+ in its interactions with the pore but its penetration of the channel inhibited by the bulky structure of the rest of the toxin.

Before studying the interactions of the toxins with the model for the Sodium channel, it was decided to investigate the interactions of the guanidinium entity with the channel pore. An optimised structure for the guanidinium ion obtained from a self-consistent field calculation using a 6-31G basis set (75) was used to calculate the interaction energy between the solvated channel and the guanidinium

fragment. The lowest interaction energy obtained was -550.88 kJ/mole and the position of the ion was found to be inside the layer of formic acid molecules and just outside the mouth of the Gramicidin-A pore as shown in figure 21. When viewed along the channel axis, the guanidinium ion was found to block the pore (figure 22). The large interaction energy in this case illustrates the possible implications of such interactions in the toxicity of the marine toxins as discussed below.

The tetrodotoxin and saxitoxin molecules were treated in a similar manner. The geometry of the former molecule was obtained from X-ray data (76) and the coordinates of saxitoxin calculated from standard geometries. The interaction energy for tetrodotoxin and saxitoxin with the pore of the refined Gramicidin-A dimer model was evaluated to be -441.14 kJ/mole and -323.57 kJ/mole. Figures 23, 24 and 25, 26 give the lateral and front views for the interactions of tetrodotoxin and saxitoxin with the mouth of the pore, respectively.

From figures 24 and 26, it is clear that in both toxins it is the guanidinium entity that preferentially interacts with the channel, blocking the transport of ions. This observation is in good agreement with the hypothesis proposed by Hille (74). Also the interaction energies for each toxin with the channel is comparable with the energetics of bond formation as listed in Table 11.

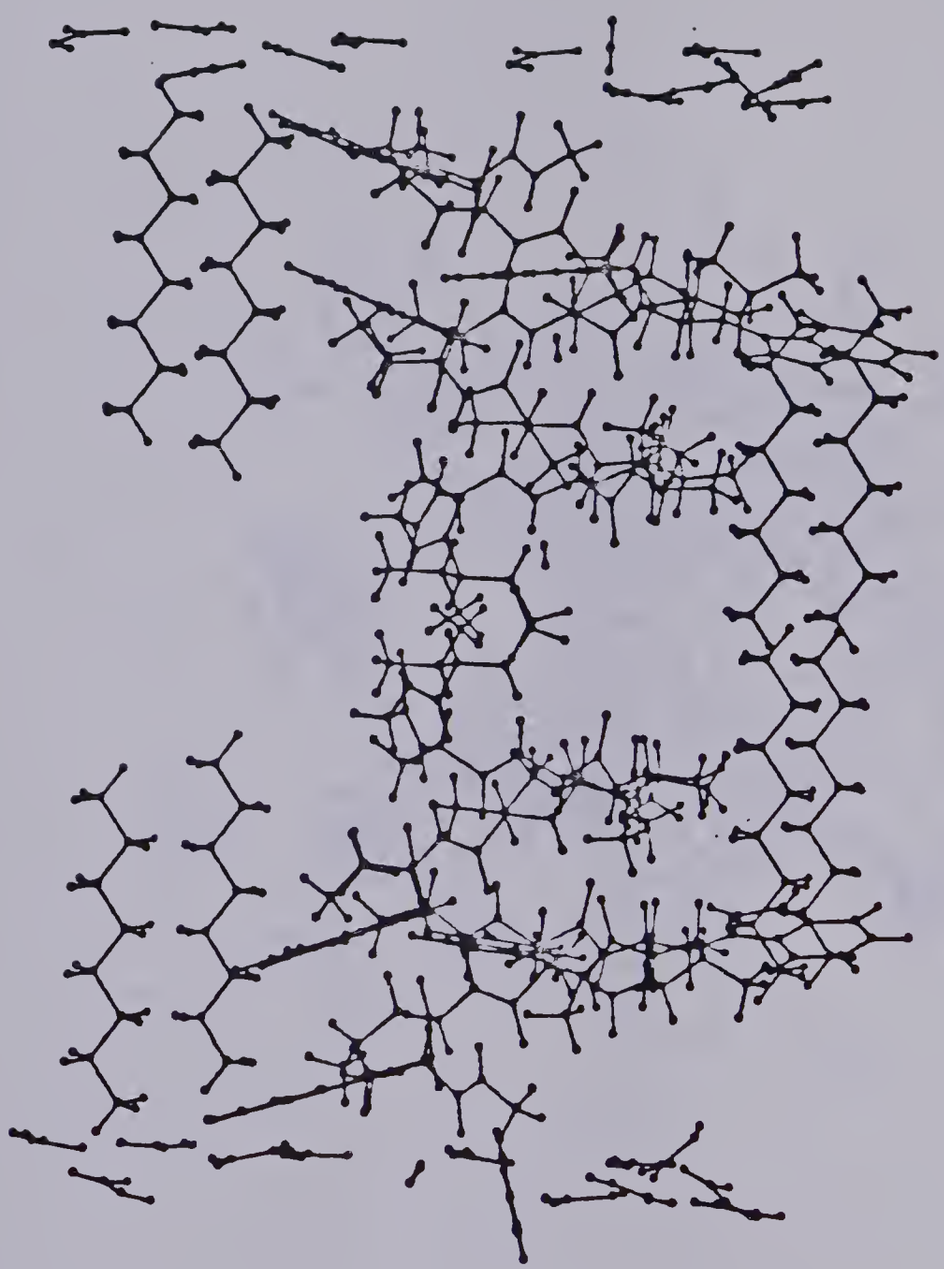

FIGURE 21 - POSITION OF THE GUANIDINIUM ION AT THE MOUTH OF THE CHANNEL.

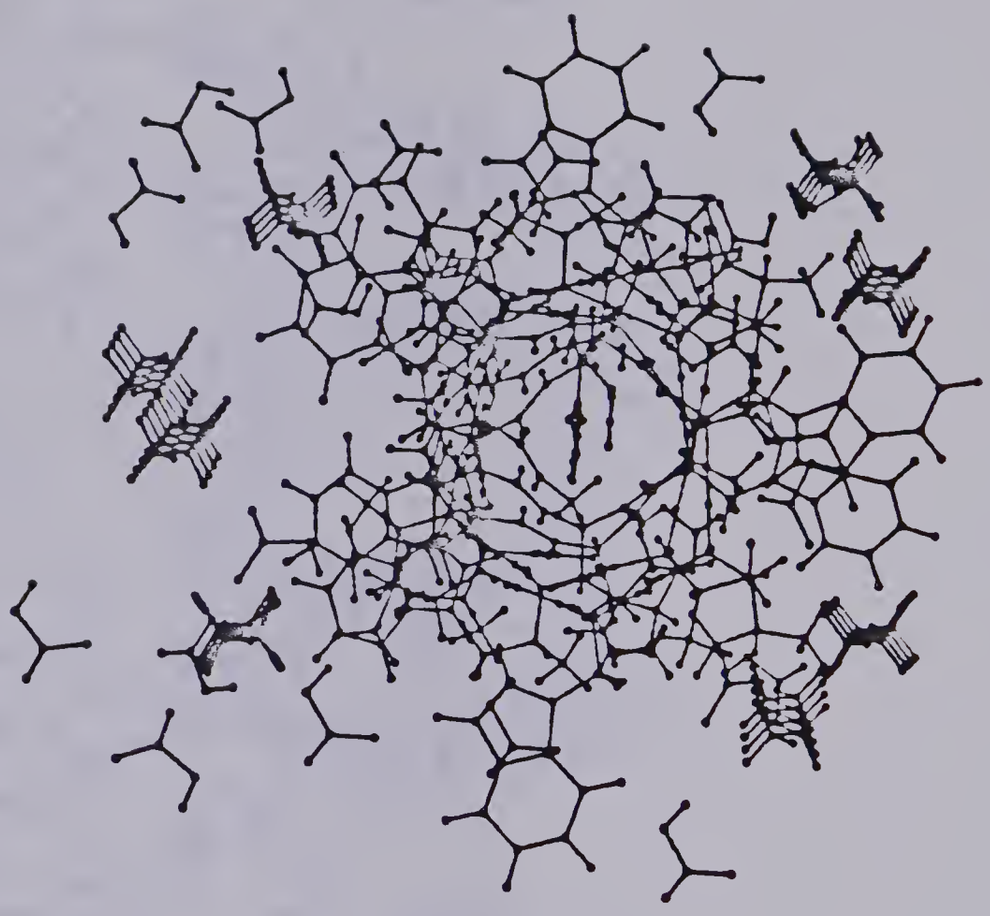

FIGURE 22 - CHANNEL BLOCKING CHARACTERISTIC OF THE GUANIDINIUM ION.

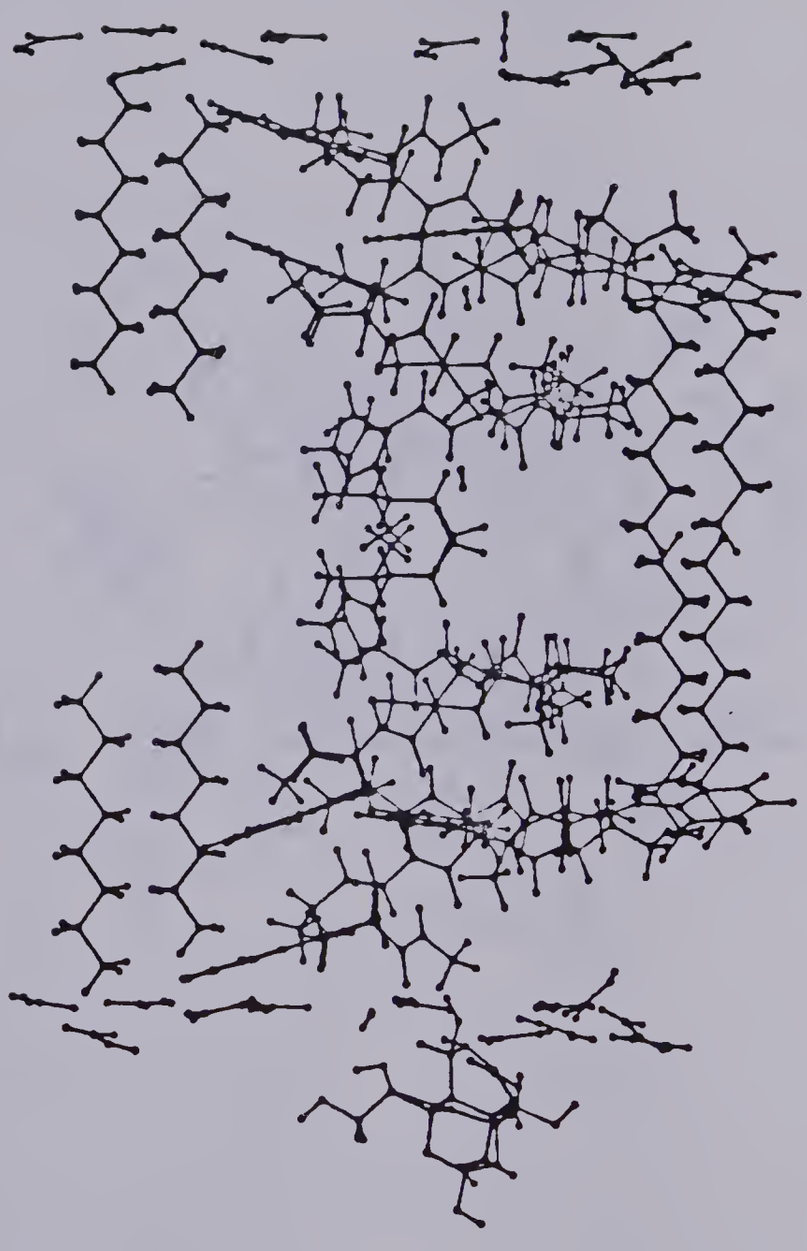

FIGURE 23 - LATERAL VIEW OF THE INTERACTION OF TETRODOTOXIN WITH THE CHANNEL.

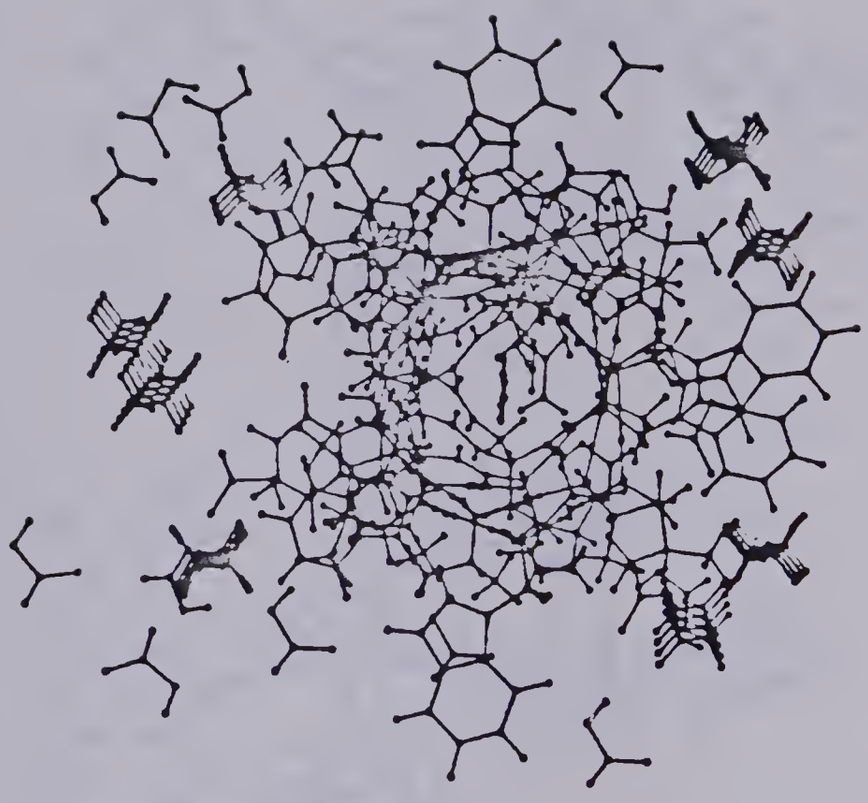

FIGURE 24 - FRONT VIEW OF THE INTERACTION OF TETRODOTOXIN WITH THE CHANNEL.

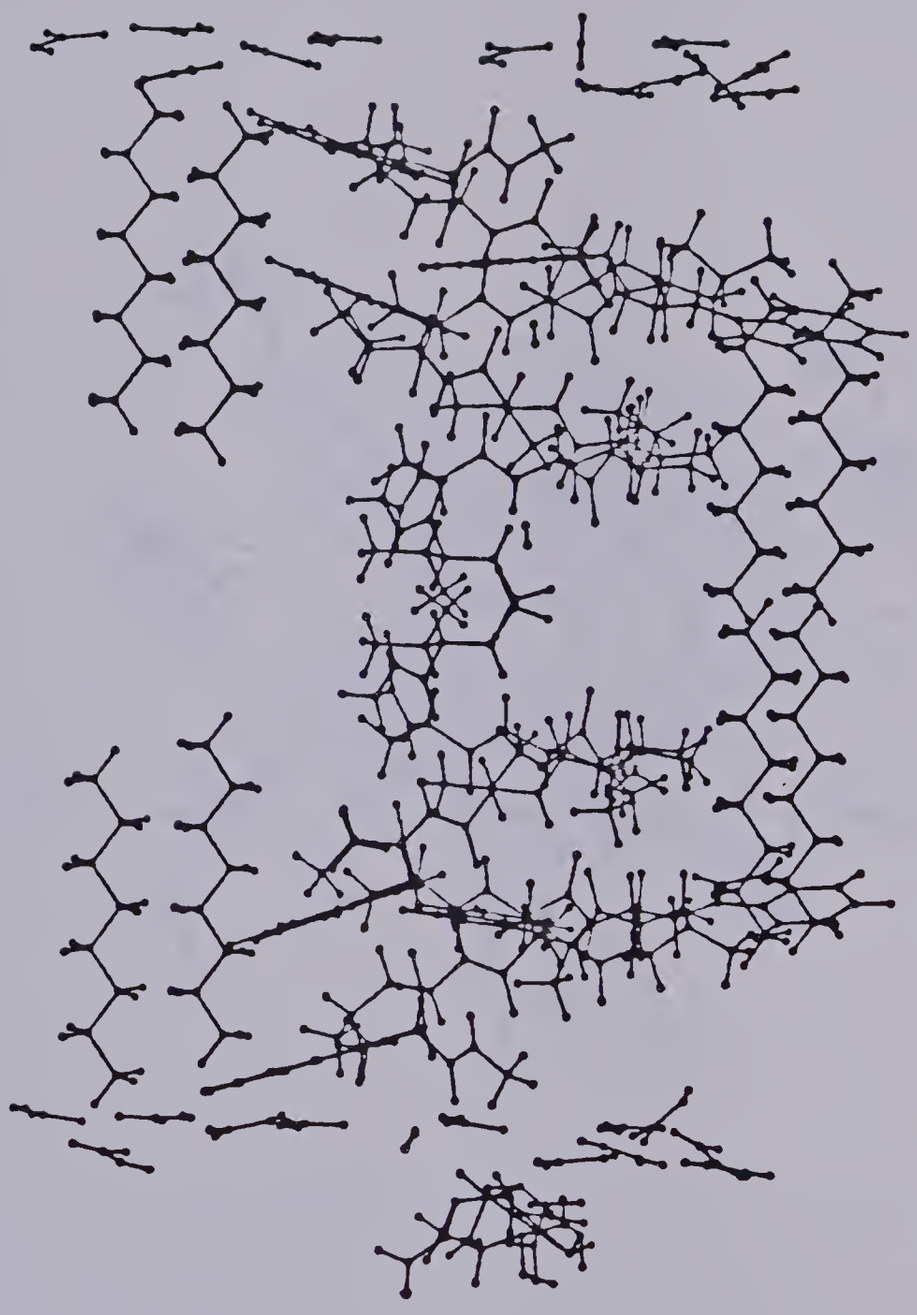

FIGURE 25 - SIDE VIEW OF THE INTERACTION OF SAXITOXIN WITH THE CHANNEL.

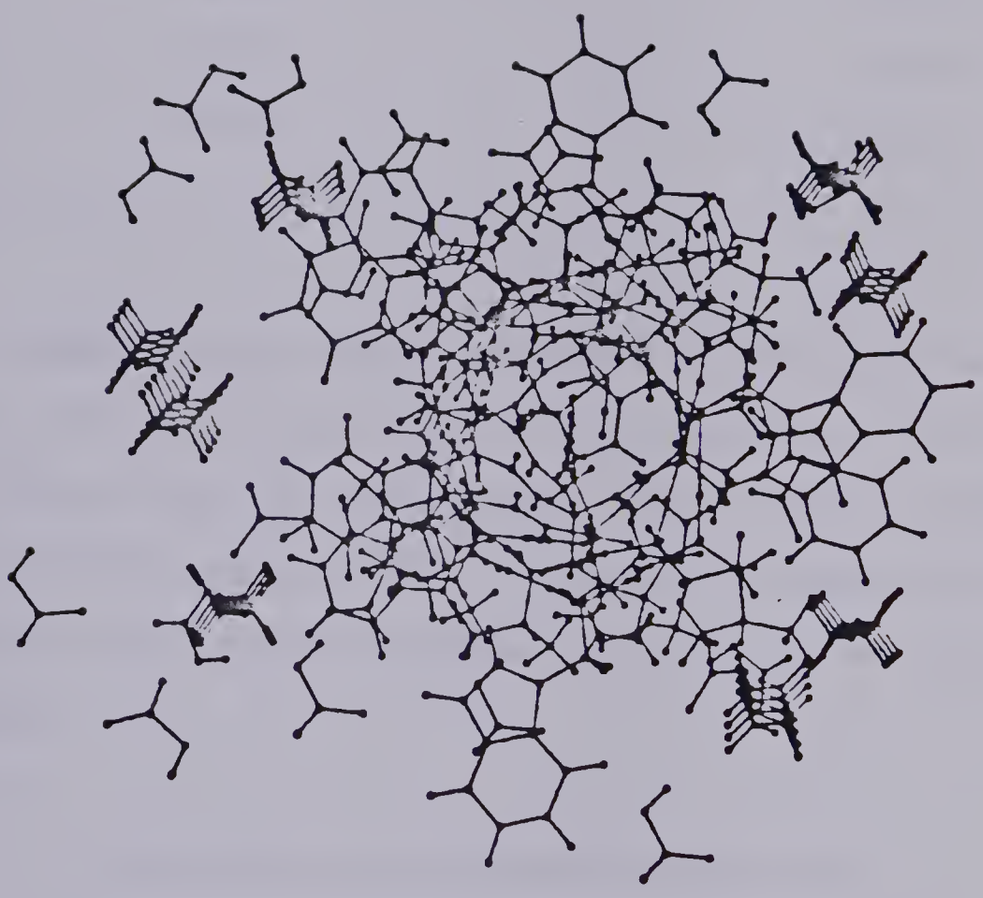

FIGURE 26 - FRONT VIEW OF THE INTERACTION OF SAXITOXIN WITH THE CHANNEL.

TABLE 11 ENERGIES FOR CERTAIN BONDS

BOND	BOND ENERGY (77) (kJ)
F-F	156.9
N-H	314.0
Me-H	435.0

Comparing the values obtained for the interaction energy of the toxins with the bond energies listed above, the interaction of these toxins with the pore of the model for the Sodium channel can certainly be classified as strong, thus illustrating the toxic nature of the two marine toxins.

3.3.2 INTERACTION OF ANESTHETIC MOLECULES

It has been postulated (9) that molecules which interfere reversibly with the conductance properties of the Sodium channel induce anesthesia. The interference could be due to a partial or complete blocking of the Sodium channel. Moreover, the interaction energy accompanying such a channel block would be expected to be in the thermal range and can be compensated by molecular collisions and conformational changes in the systems concerned.

Diethyl ether is a common anesthetic and the above hypothesis for a mechanism of anesthesia was studied by evaluating the interaction energy between the ether and the channel pore. The coordinates of the ether were obtained from X-ray crystallographic studies (78). The interaction energy of interest was obtained as in the previous cases - i.e., by specifying various positions for the ether molecule relative to the channel. The lowest energy of interaction calculated was -78.00 kJ/mole and the position of the ether molecule is as shown in figure 27. The view along the channel axis (figure 28) shows the partial blocking of the channel by diethyl ether.

The biochemical environment of the Sodium channel would have many molecules of water in the vicinity of the mouth of the pore. The incoming ether molecule has to compete with these water molecules in order to effectively block the channel. If the interaction of a molecule of ether with the mouth of the channel is more favourable than the corresponding interaction of a molecule of water, when placed at the same position as the ether, the water will be displaced by the ether.

The interaction energy for a water molecule with the pore, at the same position that gives the best energy of interaction for the ether, was evaluated to be -69.53 kJ/mole. This result shows that a molecule of ether has a preferred interaction with the channel than a water molecule

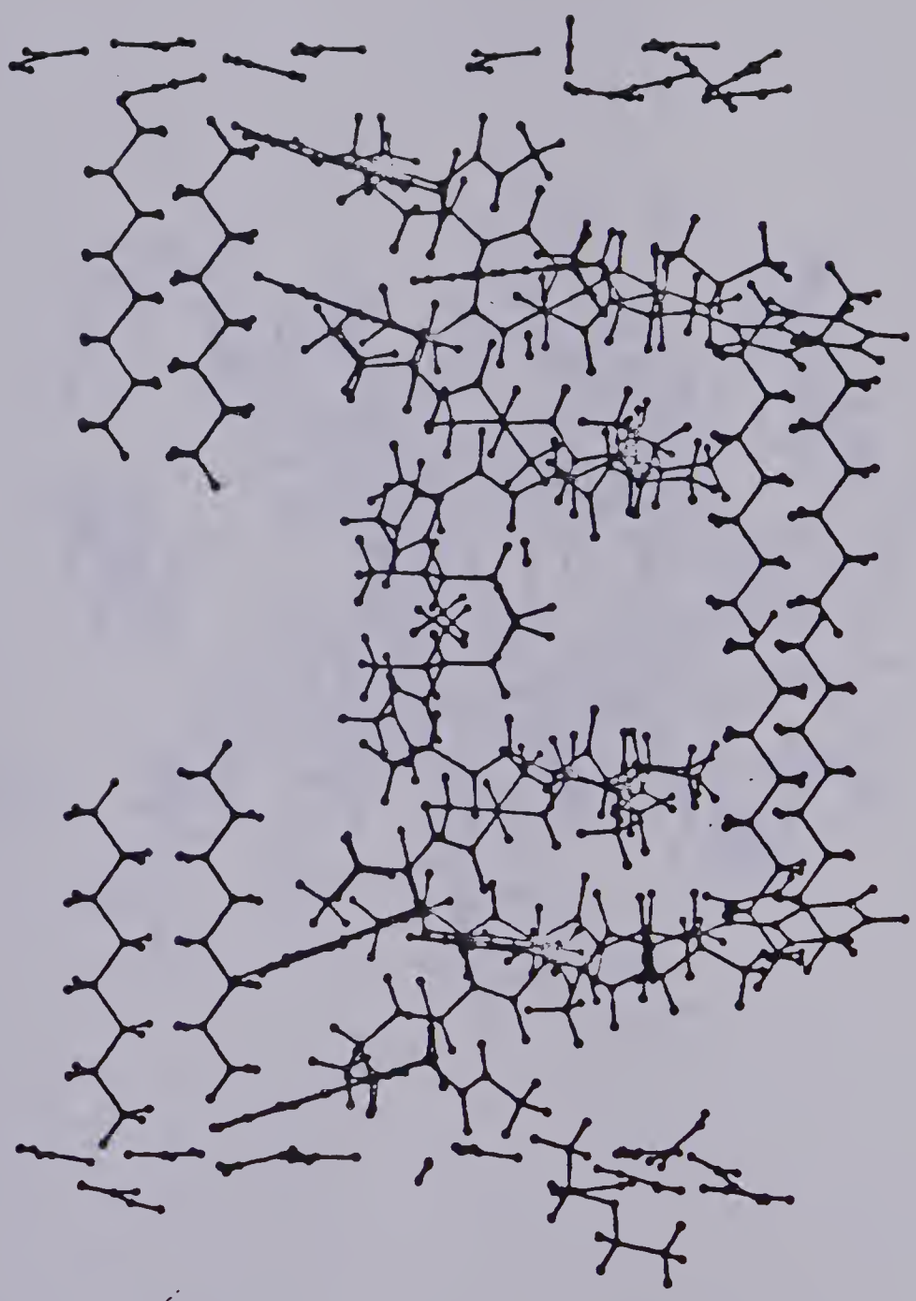

FIGURE 27 - INTERACTION OF DIETHYL ETHER WITH THE CHANNEL PORE.

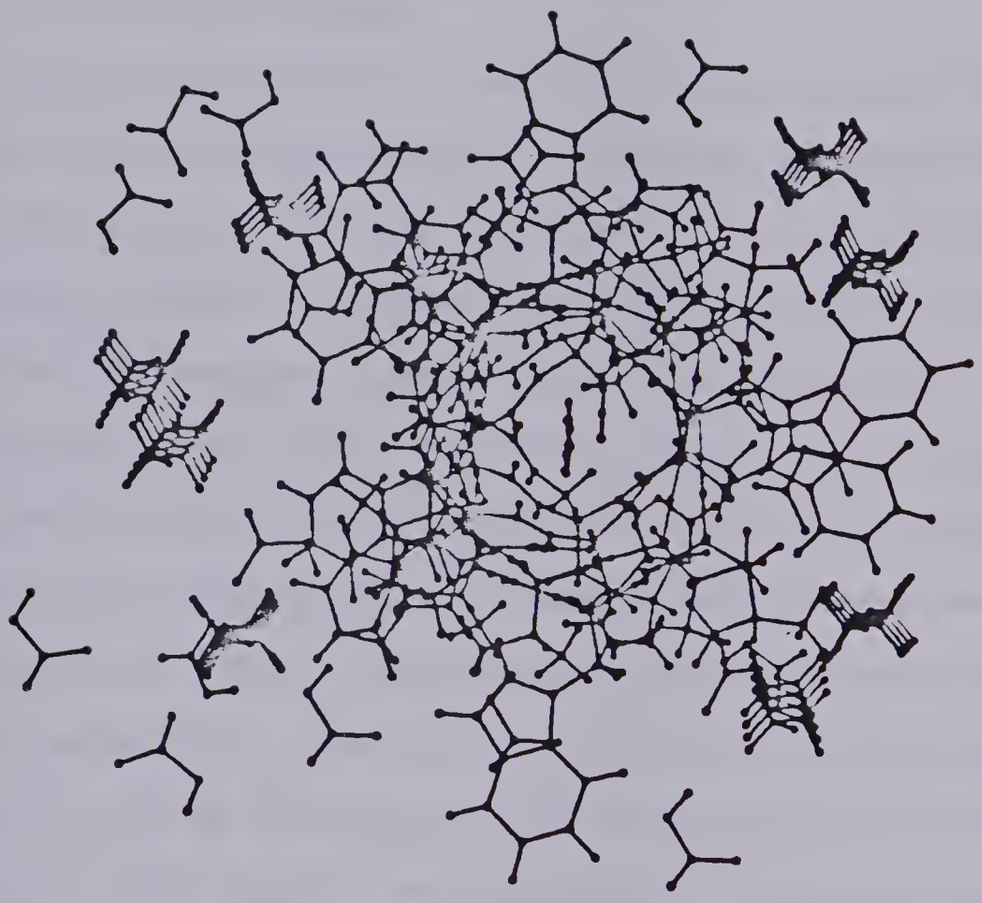

FIGURE 28 - PARTIAL BLOCKING OF THE PORE BY THE ETHER.

at that position. In other words, diethyl ether can displace water for effective interaction with the mouth of the pore. Besides, the values for the interaction energies are in the thermal range which indicates that such interactions are reversible - a requisite for a postulated mechanism of anesthesia.

Another approach in outlining a mechanism of general anesthesia is to consider the possible interactions in the synaptic cleft. Extracellular Na^+, water and, during nerve impulse, a high concentration of neurotransmitter would be some of the species found in the synaptic cleft. Interference with the conduction of the nerve impulse implies that the neurotransmitter is not available in its free form to depolarise the post-synaptic membrane. If the molecules of ether have a preferred interaction with the neurotransmitter than with water or the extracellular Sodium ions, it can be postulated that such interactions in the synaptic cleft may be responsible, in addition to the channel blocking property, for the inducement of anesthesia.

This hypothesis was tested by evaluating the energies of interaction of a Sodium ion, water and acetylcholine with a cluster of ether molecules. In each case, an ether molecule was allowed to interact with the other system (i.e., Na^+, water or acetylcholine) until the best value for the energy minimum was obtained in the steepest descent procedure. Additional ether molecules were clustered around

the initial supersystem and the energy of interaction for each new molecule evaluated.

Table 12 gives these values (in kJ/mole) for the interaction of five molecules of diethyl ether, one at a time, with Na^+, acetylcholine and water.

TABLE 12 INTERACTION ENERGIES (kJ/mole) OF Na^+, ACETYLCHOLINE AND WATER WITH DIETHYL ETHER.

SPECIES ETHER	Na^+	ACETYLCHOLINE	WATER
1	-151	-379	-33
2	-1025	-1064	-1
3	-337	-1437	
4	-455	-848	
5	-531	-281	

Although the results listed in Table 12 are preliminary by nature, there is a clear indication of the preferred interaction between the cluster of ether molecules and acetylcholine over the corresponding interactions with Na^+ or water. This trend shows that the possible interactions in the synaptic cleft should be considered along with the channel blocking property of anesthetics in formulating a mechanism of general anesthesia.

CHAPTER 4 - CONCLUSIONS

The results of the calculations presented in this thesis illustrate the applicability of a 1/R expansion in studying interactions between systems participating in biochemical processes. As the results have been discussed in the relevant sections of Chapter 3, only general comments on the applicability of the method and improvements to the theory will be presented here.

The agreement between the calculated and experimental ordering of the permeabilities of the ions improved with each refinement of the simulation of the Sodium channel. The model with the solvated pore best described the passage of the ions through the channel. Nevertheless, for the transport of Na^+, the distance between the two binding sites was not in agreement with the experimental observation of 20 Å. This may be due to many factors, among them the inadequate representation of the biological nature and environment of the channel and the neglect of the peptide libration. The introduction of peptide libration may change this parameter of ionic transport as the movement of the channel backbone to effectively coordinate the ion results in conformational changes of the Gramicidin-A dimer.

In all the results on ionic movement presented in the previous chapter, the charge on the ion is assumed to be unity for the alkali ions and two for the Calcium ion. During ionic transport, this charge may be delocalised over the amino acid residues and other molecular species, like water, present in the vicinity of the ion. Calculations (79) using the complete neglect of differential overlap (CNDO) method indicated that such charge transfers are possible and result in the stabilisation of the systems concerned.

A further refinement to the channel model would consist of replacing the simulated polar headgroups by phosphate moieties. Such a treatment requires the evaluation of the f and g parameters for phosphorous and the associated oxygen atoms. The ab-initio study (80) of the interaction of the phosphate group with water can be used to evaluate the required parameters. Simulation of the lipid environment of the ionophore by phospholipid molecules is a further improvement to the model but the computational requirements would be extremely large.

The results obtained for the interaction of the toxins with the channel illustrate the strong binding between the toxin and the mouth of the pore in agreement with recent experimental studies (81). The studies on diethyl ether illustrate some of the interactions which may be responsible for the inhibition of nervous transmission. Similar studies

on related anesthetics like methoxyflurane and isoflurane could substantiate the importance of the postulated interactions in inducing anesthesia. However, such studies require the evaluation of the f and g parameters for the Fluorine and Chlorine atoms of methoxyflurane and isoflurane. In order to determine the parameters, good ab-initio calculations for the interactions of these atoms with systems whose atoms can be assigned to known classes are required. This is the major drawback in the applicability of the method presented in this thesis.

The correlation energy defined within a variational treatment of interacting systems can be associated with the dispersion energy that can be derived in a perturbation analysis of weak interactions (82). As mentioned in section 2.2.3.2, this dispersion energy can be expressed as a function of the $(R^{-6} + R^{-8} + R^{-10})$ terms if the dipole-quadrupole and quadrupole-quadrupole contributions are considered, in addition to the dipole-dipole interaction term. Therefore, inclusion of the $(R^{-8} + R^{-10})$ terms takes into account a major portion of the intersystem correlation energy. The coefficients of these two terms would require suitable parameterisation in a manner analogous to that used for the R^{-1}, R^{-4}, R^{-6} and R^{-12} terms. The study by Lie et al (83) makes use of such a formulation together with the Hartree-Fock potential to simulate the structure of bulk water.

The applicability of the method of calculation is demonstrated by the results presented in the previous chapter of this thesis. The computational requirements are modest, even for the study of such large systems like the Gramicidin-A dimer. Within the framework of the theory, the results obtained using the potential energy function are useful in understanding interactions between biomolecules.

REFERENCES

1. A.L. Stanford Jr. "Foundations of Biophysics", Academic Press, (1975).
2. C.F. Stevens, Sci. Am. **241**, 49 (1979).
3. L. Stryer, "Biochemistry", W.H. Freeman & Co., (1981).
4. A.L. Hodgkin and A.F. Huxley, Nature (London) **144**, 710 (1939).
5. A.L. Hodgkin and A.F. Huxley, Cold Spring Harbor Symp. Quant. Biol. **17**, 43 (1952).
6. A.L. Hodgkin and A.F. Huxley, J. Physiol. (London) **116**, 449 (1952).
7. A.L. Hodgkin, A.F. Huxley and B. Katz, Arch. Sci. Physiol. 3, 129 (1949).
8. C.W. Myers and D.W. Daly, Sci. Am. **248**, 120 (1983).
9. "Molecular Mechanisms of Anesthesia", Progress in Anesthesiology, Vol. 2, Ed. B.R. Fink, Raven Press (1980).
10. M. Born and J.R. Oppenheimer, Ann. Physik, **84**, 457 (1927).
11. C.C.J. Roothan, Rev. Mod. Phys. **23**, 69 (1951).
12. F. London, Z. Phys. **63**, 245 (1930).
13. F. London, Z. Phys. Chem. B. **11**, 221 (1930).
14. F. London, Trans. Farad. Soc. **33**, 8 (1937).

15. J.O. Hirschfelder, C.F. Curtiss and R.B. Bird, "Molecular Theory of Gases and Liquids", John Wiley, New York, (1964).

16. J.E. Lennard-Jones, Proc. Roy. Soc. **A106**, 441, 463 (1924).

17. J.C. Slater and J.G. Kirkwood, Phys. Rev. **37**, 682 (1931).

18. D.R. Bates "Quantum Theory", Vol. 1, Academic Press, New York, p.280 (1961).

19. C. Mavroyannis and M.J. Stephen, Mol. Phys. **5**, 629 (1962)

20. F.A. Momany, G. Vanderkooi and H.A. Scheraga, Proc. Natl. Acad. Sc. **61**, 429 (1968).

21. F.A. Momany, R.F. McGuire and H.A. Scheraga, J. Phys. Chem. **76**, 375 (1972).

22. F.A. Momany, R.F. McGuire, A.W. Burgess and H.A. Scheraga, J. Phys. Chem. **79**, 2361 (1975).

23. F.A. Momany, L.M. Carruthers and H.A. Scheraga, J. Phys. Chem. **78**, 1621 (1974).

24. F.A. Momany, L.M. Carruthers, R.F. McGuire and H.A. Scheraga, J. Phys. Chem. **78**, 1595 (1974).

25. J.A. Pople, D.A. Santry and G.A. Segal, J. Chem. Phys., **43**, S129 (1965).

26. W.P. Minicozzi and D.F. Bradley, J. Compt. Phys. **4**, 118 (1969).

27. T. Ooi, R.A. Scott, G. Vanderkooi and H.A. Scheraga, J. Chem. Phys. **46**, 4410 (1967).

28. E. Clementi, F. Cavallone and R. Scordamaglia, J. Am. Chem. Soc. **99**, 5531 (1977).

29. R. Scordamaglia, F. Cavallone and E. Clementi, J. Am. Chem. Soc. **99**, 5545 (1977).

30. G. Bolis and E. Clementi, J. Am. Chem. Soc. **99**, 5550 (1977).

31. E. Clementi, Int. J. Quant. Chem. **3S**, 179 (1970).

32. Technical Report TC-AR-I-81, Division of Theoretical Chemistry, Department of Chemistry, The University of Alberta (1981).

33. S. Fraga, J. Comp. Chem. **3**, 329 (1982).

34. G. Corongiu, E. Clementi, E. Pretsch and W. Simon, J. Chem. Phys. **70**, 1266 (1979).

35. H. Popkie and E. Clementi, J. Chem. Phys. **57**, 1077 (1972).

36. H. Kistenmacher, H. Popkie and E. Clementi, J. Chem. Phys. **58**, 1689 (1973).

37. H. Tatewaki and S. Huzinaga, J. Comp. Chem. **1**, 205 (1980).

38. S. Fraga, K.M.S. Saxena and J. Karwowski, "Hartree-Fock Atomic Data" (1975).

39. S.F. Boys and F. Bernadi, Mol. Phys. **19**, 553 (1970).

40. A. Johansson, P. Kollman, S. Rothenberg, Theor. Chim. Acta **29**, 167 (1973).

41. S. Fraga, Computer Physics Communications (in press).

42. R.S. Keynes, Sci. Am. **103**, 126 (1979).

43. J.B. Chappel and A.R. Gofts, Biochem. J. **95**, 393 (1965).

44. E.J. Harris and B.C. Pressman, Nature (London) **216**, 918 (1967).

45. P. Mueller and D.O. Rudin, Biochem. Biophys. Res. Commun. **26**, 398 (1967).

46. S.B. Hladky and D.A. Haydon, Biochim. Biophys. Acta **274**, 294 (1972).

47. D.C. Tosteson, T.E. Andreoli, M. Tieffenberg and P. Cook, J. Gen. Physiol. **51**, 373S (1968).

48. W.R. Veatch, R. Mathies, M. Eisenberg and L. Stryer, J. Mol. Biol. **99**, 75 (1975).

49. W.R. Veatch and L. Stryer, J. Mol. Biol. **113**, 89 (1977).

50. D.W. Urry, M.C. Goodall, J.D. Glickson and D.F. Mayers, Proc. Nat'l. Acad. Sci. U.S.A. **68**, 1907 (1971).

51. E. Bamberg and K. Janko, Biochim. Biophys. Acta **465**, 486 (1977).

52. R. Sarges and B. Witkop, J. Am. Chem. Soc. **87**, 2011 (1965).

53. D.W. Urry, Proc. Nat'l. Acad. Sci. U.S.A. **68**, 672 (1971).

54. R.J. Bradley, D.W. Urry, K. Okamoto and R. Rapaka, Science **200**, 435 (1978).

55. W.R. Veatch, E.T. Fossel and E.R. Blout, Biochemistry **13**, 5249 (1974).

56. W.R. Veatch and E.R. Blout, Biochemistry **13**, 5257 (1974).

57. S. Weinstein, B.A. Wallace, E.R. Blout, J.S. Morrow and W. Veatch, Proc. Nat'l. Acad. Sci. U.S.A. **76**, 4230 (1979).

58. D.W. Urry, C.M. Venkatachalam, K.U. Prasad, R.J. Bradley, G. Parenti-castelli and G. Lenaz, Int. J. Quantum Chem. Quantum Biol. Symp. **8**, 385 (1981).

59. M. Jean Browman, Lucy M. Carruthers, Karen L. Kashuba, Frank A. Momany, Marcia S. Pottle, Susan P. Rosen, Shirley M. Rumsey, QCPE (Prog. no. 286) (1975).

60. B. Maigret and B. Pullman, Theoret. Chim. Acta **35**, 113 (1974).

61. B. Maigret, D. Perahia and B. Pullman, Biopolymers **10**, 491 (1971).

62. E.T. Hesselnik and H.A. Scheraga, Macromolecules **5**, 455 (1972).

63. D.W. Urry, T.L. Trapane and K.U. Prasad, Int. J. Quantum Chem. Quantum Biol. Symp. **9**, 31 (1982).

64. R. Koeppe, K. Hodgson and L. Stryer, J. Mol. Biol. **121**, 41 (1978).

65. V.B. Myers and D.A. Haydon, Biochim. Biophys. Acta **274**, 313 (1972).

66. D.W. Urry "Conformation of Biological Molecules and Polymers", Jerusalem Symposia on Quantum Chemistry and Biochemistry, Vol V, (Israel Academy of Sciences, Jerusalem) p.723 (1973).

67. D.W. Urry, C.M. Venkatachalam, A. Spisni, P. Läuger and M.A. Khaled, Proc. Nat'l. Acad. Sci. U.S.A. **77**, 2028 (1980).

68. D.W. Urry, C.M. Venkatachalam, A. Spisni, R.J. Bradley, T.L. Trapane and K.U. Prasad, J. Membr. Biol. **55**, 29 (1980).

69. C.M. Venkatachalam and D.W. Urry, J. Magn. Res. **41**, 313 (1980).

70. Inger Nahringbauer, Acta. Cryst. **B34**, 315 (1978).

71. D.W. Urry, A. Spisni, M.A. Khaled, M.M. Long and L. Masotti, Int. J. Quantum Chem., Quantum Biol. Symp., **6**, 289 (1979).

72. A. Finkelstein, "Drugs and Transport Processes", Ed. B.A. Canningham, Macmillan, p.241 (1974).

73. R.E. Koeppe II, J.M. Berg, K.O. Hodgson and L. Stryer, Nature (London) **279** 723 (1979).

74. B. Hille, Biophys. J. **22**, 283 (1978).

75. A.M. Sapse and A. Santoro, J. Comp. Chem. **2**, 363 (1981).

76. A. Furusaki, the late Y. Tomiie and I. Nitta, Bull. Chem. Soc. Jap. **43**, 3332 (1970).

77. C.R.C. Handbook of Chemistry & Physics, 60th Edition, CRC Press (1979-1980).

78. D. André, R. Fourme and K. Zechmeister, Acta Cryst., **B28**, 2389 (1972).

79. V. Renugopalakrishnan and D.W. Urry, Biophys. J. **24** 729 (1978).

80. E. Clementi, G. Corongiu and F. Lelj, J. Chem. Phys. **70**, 3726 (1979).

81. J.M. Ritchie and H.P. Rang, Proc. Nat'l Acad. Sci. **80**, 2803 (1983).

82. P. Hobza and R. Zahradnik "Weak Intermolecular Interactions in Chemistry and Biology", Elsevier Scientific Publishing Company (1980).

83. G.C. Lie and E. Clementi, J. Chem. Phys. **62**, 2195 (1975).